Pergamon

Geochimica et Cosmochimica Acta, Vol. 68, No. 9, pp. 1989–2006, 2004

0016-7037/04 $30.00 + .00

doi:10.1016/j.gca.2003.09.021

The origin and mechanisms of salinization of the Lower Jordan River

EFRAT FARBER,[1] AVNER VENGOSH,[1,*] ITTAI GAVRIELI,[2] AMER MARIE,[3] THOMAS D. BULLEN,[4] BERNHARD MAYER,[5] RAN HOLTZMAN,[6] MICHAL SEGAL,[6] and URI SHAVIT[6]

[1]Department of Geological and Environmental Sciences, Ben Gurion University, Beer Sheva 84105 Israel
[2]Geological Survey of Israel, Jerusalem 95501, Israel
[3]Department of Applied Earth and Environmental Sciences, Al-Quds University, East Jerusalem, West Bank, Palestine
[4]Water Resources Division, U.S. Geological Survey, Menlo Park, California 04025 USA
[5]Department of Physics & Astronomy and Department of Geology & Geophysics, University of Calgary, Calgary, Alberta T2N 1N4 Canada
[6]Department of Civil and Environmental Engineering, Technion, Israel Institute of Technology, Haifa 32000 Israel

(*Received April* 25, 2003; *accepted in revised form September* 29, 2003)

Abstract—The chemical and isotopic ($^{87}Sr/^{86}Sr$, $\delta^{11}B$, $\delta^{34}S_{sulfate}$, $\delta^{18}O_{water}$, $\delta^{15}N_{nitrate}$) compositions of water from the Lower Jordan River and its major tributaries between the Sea of Galilee and the Dead Sea were determined in order to reveal the origin of the salinity of the Jordan River. We identified three separate hydrological zones along the flow of the river:

(1) A northern section (20 km downstream of its source) where the base flow composed of diverted saline and wastewaters is modified due to discharge of shallow sulfate-rich groundwater, characterized by low $^{87}Sr/^{86}Sr$ (0.7072), $\delta^{34}S_{sulfate}$ (−2‰), high $\delta^{11}B$ (~36‰), $\delta^{15}N_{nitrate}$ (~15‰) and high $\delta^{18}O_{water}$ (−2 to–3‰) values. The shallow groundwater is derived from agricultural drainage water mixed with natural saline groundwater and discharges to both the Jordan and Yarmouk rivers. The contribution of the groundwater component in the Jordan River flow, deduced from mixing relationships of solutes and strontium isotopes, varies from 20 to 50% of the total flow.

(2) A central zone (20–50 km downstream from its source) where salt variations are minimal and the rise of $^{87}Sr/^{86}Sr$ and SO_4/Cl ratios reflects predominance of eastern surface water flows.

(3) A southern section (50–100 km downstream of its source) where the total dissolved solids of the Jordan River increase, particularly during the spring (70–80 km) and summer (80–100 km) to values as high as 11.1 g/L. Variations in the chemical and isotopic compositions of river water along the southern section suggest that the Zarqa River ($^{87}Sr/^{86}Sr$~0.70865; $\delta^{11}B$~25‰) has a negligible affect on the Jordan River. Instead, the river quality is influenced primarily by groundwater discharge composed of sulfate-rich saline groundwater (Cl^-=31–180 mM; SO_4/Cl~0.2–0.5; Br/Cl~2–3×10^{-3}; $^{87}Sr/^{86}Sr$~0.70805; $\delta^{11}B$~30‰; $\delta^{15}N_{nitrate}$ ~17‰, $\delta^{34}S_{sulfate}$=4–10‰), and Ca-chloride Rift valley brines (Cl^-=846–1500 mM; Br/Cl~6–8×10^{-3}; $^{87}Sr/^{86}Sr$~0.7080; $\delta^{11}B$>40‰; $\delta^{34}S_{sulfate}$=4–10‰). Mixing calculations indicate that the groundwater discharged to the river is composed of varying proportions of brines and sulfate-rich saline groundwater. Solute mass balance calculations point to a ~10% contribution of saline groundwater (Cl^-=282 to 564 mM) to the river. A high nitrate level (up to 2.5 mM) in the groundwater suggests that drainage of wastewater derived irrigation water is an important source for the groundwater. This irrigation water appears to leach Pleistocene sediments of the Jordan Valley resulting in elevated sulfate contents and altered strontium and boron isotopic compositions of the groundwater that in turn impacts the water quality of the lower Jordan River.

1. INTRODUCTION

River salinization is a phenomenon that has shaped human history at least since the fourth millennium BC. New evidence suggests that the rise and collapse of early civilizations (e.g., the Akkadian, 4200 BP.) were affected by the salinization of their rivers (e.g., the Tigris and Euphrates rivers (Cullen et al., 2000; deMenocal, 2001)). While prehistoric salinization is associated with both climatic changes and man's activity through irrigation practice, modern salinization is caused primarily by direct and indirect human activities. The water quality of many rivers in arid and semiarid areas is deteriorating due to a combination of extensive land use changes, diversion and damming of rivers, generation of saline agricultural return flows, and sewage dumping. The results are striking; the rise of salt content causes a decrease in biodiversity, a replacement of the halo-sensitive biota with halo-tolerant species, soil salinization, and diminishing of water resources (Williams, 2001). The dominant factor determining the quality of rivers in water scarce areas is the balance between freshwater withdrawal, groundwater discharge, and agricultural return flow. As more fresh surface water is diverted, the impact of the agricultural return flow increases (Pillsbury, 1981).

The rise of salt content in rivers such as the Colorado and the Arkansas Rivers in the United States is derived from a combination of upstream diversion of fresh water, intensive irrigation, and formation of saline agricultural return flow, which enters the river (Pillsbury, 1981; Gates et al., 2002). Similarly, saline agricultural drainage increases the salt contents of the Nile (Kotb et al., 2000), Euphrates, and Tigris rivers (Robson et al., 1983; Beaumont, 1996). In contrast,

* Address reprint requests to Dr. A. Vengosh, Department of Geological and Environmental Sciences, Stanford University, Braun Hall, Bldg. 320, Rm. 228, Stanford, CA 94305-2115 (avnerv@bgumail.bgu.ac.il).

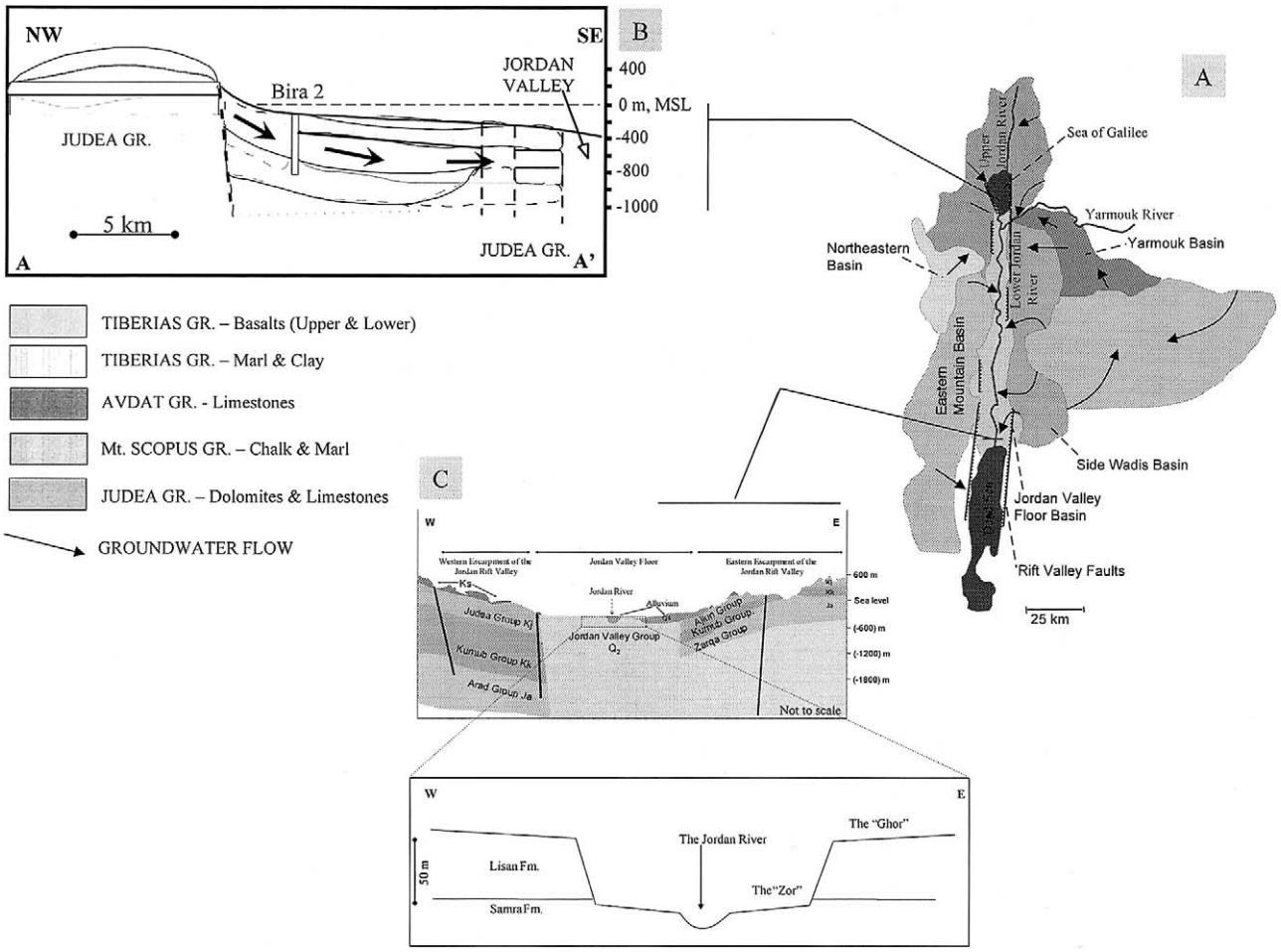

Fig. 1. A-Groundwater basins and groundwater flow direction (indicated by arrows) in the Jordan Valley and vicinity; B-A schematic geological cross section in the northern the Jordan Valley (from Möller et al., 2003); C-A schematic hydrogeological cross section in the southern Jordan Valley (after Exact; 1998); D-A shallow morphologic structure in Abdalla Bridge site.

the source of the dissolved salts of the Murray River in South Australia (Allison et al., 1990; Herczeg et al., 1993) and the Rio Grande in the United States (Phillips et al., 2002), is geogenetic and derived from discharge of saline groundwater. In spite of the importance of river salinization in dryland environments, only a few studies have investigated the full chemical and isotopic compositions of salinized rivers (e.g., Herczeg et al., 1993; Phillips et al., 2002).

Here we examine the water quality of the Jordan River and its tributaries between the Sea of Galilee (Lake Tiberias, Lake Kineret) and the Dead Sea (Fig. 1). We determined the chemical compositions, water isotope (oxygen), and solute isotope (strontium, boron, sulfur, nitrogen) compositions of river, inflows, and groundwater samples to evaluate the sources and mechanisms of inflow of solutes dissolved in the river. We show that the integration of chemical and isotopic tracers with solute mass balance calculations can be used to delineate the different salt sources and to quantify their impact on the water quality of the Jordan River.

2. ANALYTICAL TECHNIQUES

Seventy sites were selected on the Jordan River and its tributaries at both sides of the Jordan River, between the Sea of Galilee and the Dead Sea (Fig. 2). The sites were sampled throughout the hydrological yr to monitor seasonal variations. Overall, 520 water samples were collected during 14 field trips to the Jordan Valley between September 1999 and August 2001. Water samples were collected in new plastic bottles that were rinsed several times with the sample waters before storage. Samples were collected in separate bottles for chemical, solute isotope (B, Sr, S, N), and oxygen isotope analyses, respectively. Samples that were analyzed for solute content and isotopes were filtered (0.45μ) within 24 to 48 h after sampling. After sampling, the samples were stored at 4°C, both in the field and in the laboratory.

The samples were analyzed for major and minor ions (all samples) at the Geological Survey of Israel. Cation and boron concentrations were measured by inductively coupled plasma–optical emission spectrometry (ICP-OES), anion concentrations by ion chromatography (IC), and bicarbonate by titration. The imbalance between positive and negative charged ions did not exceed 5%, which reflects the overall precision of the analytical procedures. Isotope ratios of strontium (n = 77), boron (n = 97), sulfur in sulfate (n = 31), oxygen in water (n = 164), and nitrogen in nitrate (n = 18) were also determined. Strontium was separated from the waters by ion exchange using Biorad AG50X8 resin at Ben-Gurion University. Sr isotope ratios were determined by thermal

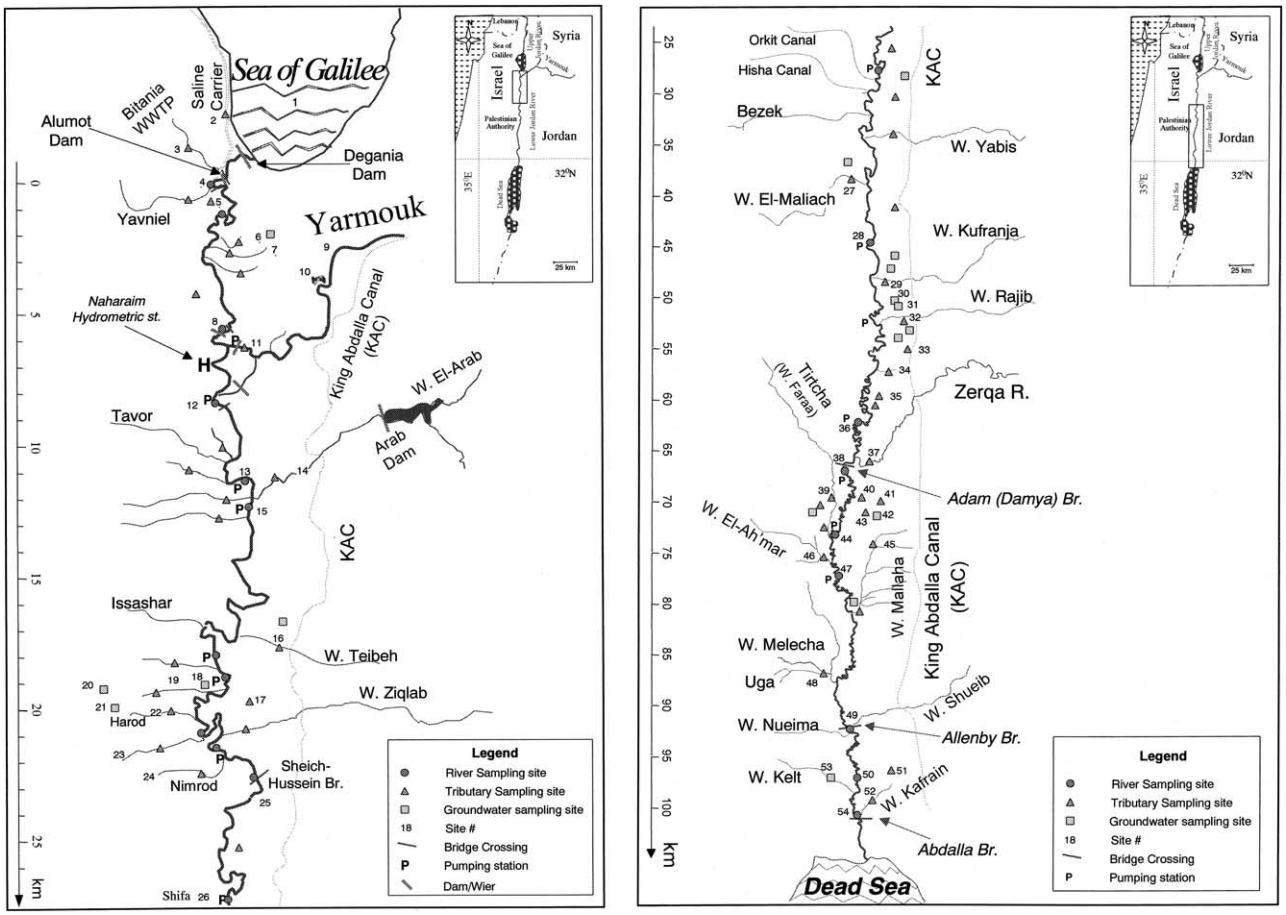

Fig. 2. Detailed maps of the northern (A) and southern (B) parts of the lower Jordan River. Sampling points along the river, inflows and shallow boreholes are marked and listed in Table 2.

ionization mass spectrometry at the U.S. Geological Survey, Menlo Park, California, USA. An external precision of 2×10^{-5} for the Sr isotope measurements was determined by replicate analyses of the N.I.S.T. 987 Sr metal standard. Laboratory preparation and mass spectrometry procedures are identical to those described in Bullen et al. (1996). Boron isotope ratios were measured by negative thermal ionization mass spectrometry (direct loading procedure; Vengosh et al., 1991b) at the U.S. Geological Survey, Menlo Park, California, USA. For each water sample, an aliquot containing approximately 2 ng of boron was evaporated on a rhenium filament. For mass spectrometry all samples were ionized at 950–1000°C, and each sample was analyzed in duplicate. The measured $^{11}B/^{10}B$ ratios were normalized to the N.I.S.T. 951 boric acid standard. At the Menlo Park laboratory, $\delta^{11}B$ of seawater is +39.2 ‰ relative to this standard. External analytical reproducibility of boron isotope ratios is 1‰, based on replicate analyses of the N.I.S.T. 951 and seawater standards, and duplicate measurements of individual samples. For $\delta^{34}S$ analyses, SO_2 gas was produced and collected on a vacuum line in the Geological Survey of Israel, following the procedure described by Coleman and Moore (1978) (Gavrieli et al., 2001). Isotopic measurements of the SO_2 gas were done at the British Geological Survey, Keyworth, UK. The $\delta^{34}S$ values are reported in per mil relative to the CDT standard. Reproducibility of gas preparation and isotope measurements for an internal laboratory standard was ±0.2‰ over a time period of 5 yrs (n = 140). NBS-127 $\delta^{34}S$=20.3 ± 0.2‰; n = 7) was used to calibrate the internal standard. The determination of $\delta^{18}O$ values of water was carried out using the triple collector VG SIRA-II mass spectrometer at the Geological Survey of Israel. The $\delta^{18}O$ values are reported in per mil relative to SMOW (Craig, 1961). The analytical precision is 0.01‰, and the external reproducibility of three-four duplicates of standards in each run is better than 0.1‰. For measurements of nitrogen isotope ratios of dissolved nitrate in the water, SO_4^{2-} was removed by precipitation as $BaSO_4$ and HCO_3^- by adjusting the pH to less than 4. Nitrate was separated using an ion exchange resin technique described by Silva et al. (2000). Subsequently, nitrate was converted to $AgNO_3$ at the University of Calgary (Alberta, Canada). Nitrogen isotope ratios were determined on N_2 after thermal decomposition of $AgNO_3$ in an elemental analyzer and subsequent continuous-flow isotope ratio mass spectrometry. $\delta^{15}N$ values for all samples were calibrated against international reference materials (IAEA N1 and N2). The overall reproducibility of nitrate extraction, gas preparation, and mass spectrometric measurements was better than ±0.5 ‰ based on replicate analyses (n = 10) of saline water samples.

3. HYDROLOGY AND HYDROGEOLOGY

The Jordan River exhibits a range of total dissolved solid contents of between a few mg/L upstream of the Sea of Galilee to thousands of mg/L before its confluence to the Dead Sea (Fig. 1). The historical annual discharge of the Jordan River was ~1300 million cubic meter (MCM) per yr (Hof, 1998; Klein, 1998; Salameh and Naser, 1999). It included water from the Sea of Galilee (Lake Tiberias ~540 MCM/yr), the Yarmouk River (~500 MCM/yr), and local runoff (Fig. 2). After damming Lake Tiberias its outflow almost totally ceased. Water is released to the Lower Jordan River only on rare occasions of extremely wet years. To reduce the salt contents of Lake

Tiberias, natural saline springs in its vicinity (e.g., the thermal Tiberias springs) are diverted through the "saline water carrier" to the Lower Jordan River (15 to 20 MCM/yr). Together with sewage effluents (~10 MCM/yr), the saline water carrier currently forms the primary water source of the Lower Jordan River. The discharge of the Yarmouk River (Fig. 2) to the Jordan River has been drastically reduced due to water diverted via the King Abdalla Canal to Jordan (150 MCM; Klein, 1998) and upstream water use in Syria. Accordingly, the current contribution from the fresh Yarmouk to the Jordan River is nearly zero and the water downstream from Adassia Dam that enters to the Jordan River is saline. Other water sources that flow to the Lower Jordan River comprise drainage of fishponds, wastewater, fresh and saline springs, and agricultural return flows. At present, only 50–200 MCM/yr of mostly poor quality fluids reach the Dead Sea through the Lower Jordan River. This dramatic reduction in water flow during the last few decades has resulted in a significant degradation of river water quality (Hof, 1998; Klein, 1998). Archival data (from Bentor, 1961; Neev and Emery, 1967) reveal that at Abdalla Bridge, in the most southern point of the Jordan River, chloride contents were ~11 mM between 1925 and 1947 but have increase to >85 mM at present. The most eminent outcome of the dramatic reduction in the discharge of the Jordan River, which is the main water source of the Dead Sea, is the >20 m decline in the Dead Sea water level over the last decades (Yechieli et al., 1998).

The Central Jordan Rift Valley is a pull-apart basin, with a width of 5–9 km in the north to 23 km in the south (Fig. 1). Its eastern and western boundaries are the escarpment caused by the faults of the Rift. The valley drains groundwater that flows from adjacent basins. In the northern part, groundwater flows primarily from basaltic aquifers, one on the western side (Tiberias Group; Möller et al., 2003), and one is part of the Yarmouk basin on the eastern side (Fig. 1). On the western side of the Jordan Rift Valley, groundwater flows also from calcareous aquifers (Judea, Mt. Scopus and Avdat Groups). On the eastern side, groundwater flows from the Ajloun Highland mainly via the Campanian limestone (B2) and Turonian (A7) aquifers (Bajjali et al., 1997).

In most parts of the Jordan Valley, the western component of groundwater that flows to the Jordan Valley is from the Eastern and Northeastern Mountain basins that are composed of calcareous Cenomanian (Judea group) and Eocene (Avdat Group) rocks (Fig. 1). Along the eastern fault escarpment, three major aquifer systems are identified (1) Amman-Wadi Sir (Ks) aquifer (Upper Cretaceous to Paleocene limestone and chert of Belqa Group); (2) Hummer (Kj) aquifer (Upper Cretaceous dolomitic limestone of Ajlun Group); and (3) Kurnub (Kk, Lower Cretaceous) and Zarqa (Ja-Jurassic) aquifers (Salameh 1996; Exact, 1998).

The Jordan River is incised into Pleistocene sediments that fill the Rift valley. In the northern section the sediments are composed of marls, sand, conglomerate, calcite, and diatomite (Hazan, 2003). In the southern part (40 km from the Sea of Galilee) the sediments are composed of the Late Pleistocene Lisan Formation (alteration of aragonite, marls, detrital and gypsum layers) overlying the Neogene–Pleistocene Samra Formation (alternation of marls, sand, conglomerate, oolitic limestone, chalk (Begin et al., 1974; Landmann et al., 2002; Waldmann, 2002)). Along the entrances of side wadis into the Jordan Valley, the lithological composition is altered by alluvial and detritus sediments (e.g., sand, conglomerate). The relatively high conductivity of the detritus sediments results in formation of local aquifers (e.g., Jericho area; Gropius and Klingbeil, 1999; Marie and Vengosh, 2001). In the northern part, the association of basaltic rocks along both sides of the valley (Fig. 1) resulted in formation of basalt gravels within the Jordan Valley. In the central and southern parts, the compositions of the alluvial materials mimic those of the rocks along both sides of the valley. The morphologic structure of the Jordan Valley is composed of the present flood plain of the Jordan River (the "Zor") and past flood plains at higher elevations (the "Ghor"). In most cases, the modern Jordan River and thus the "Zor" area is incised in the underlying Samra Formation where the upper Ghor plain is composed of the Lisan Formation, and in some cases also the Holocene Zeelim (Damia) Formation (Fig. 1D; Landmann et al., 2002).

4. RESULTS AND DISCUSSION

The chemical and isotopic compositions of water from the Jordan River, its major tributaries, and groundwater resources in the Jordan Valley are presented in Table 1. Summary of the characteristics of the major water sources that flow to the Jordan Valley are presented in Table 2. We identified three river sections in terms of salt content variation along the Lower Jordan River (Fig. 3): an upper (northern) section, where the initial high salt content decreases downstream; a middle section, where the dissolved salt variation is less significant; and a lower (southern) section, where salt content increases downstream. Together with the salt content changes we observed chemical and isotopic variations along the river flow (Fig. 3). We hypothesize that at least three processes can account for changing the chemical and isotopic compositions of the river water: (1) net evapotranspiration that would increase the content of conservative solutes downstream. If this is the only process, the ionic ratios and isotopic compositions of conservative constituents in the downstream river segments should be identical to those of the upstream river. (2) Inflows from tributaries (point sources) that modify the river water composition in a step-like function. In this case, the river water composition is modified in accordance to the relative contribution of the inflows. (3) Groundwater discharge (i.e., a non-point source), in which the river water composition is gradually modified along the flow due to an increasing fraction of the groundwater component. The composition of conservative constituents in the downstream river should reflect the relative contribution of the inflowing groundwater. We will now examine these hypotheses in light of the water quality changes observed along the three sections of the Jordan River.

4.1. Chemical Modification in the Northern Section

The initial base flow (~30 MCM/yr) of the Jordan River (Alumot Dam, Table 2 and Fig. 2) comprises a mix of diverted saline spring water, referred to as the "saline water carrier," (chloride range of 56 to 78 mM), wastewater from the city of Tiberias, and poorly treated sewage effluents (7 to 13 mM). A blend of these source waters is dumped to the river. Based on

Table 1. The chemical and isotopic compositions of representative samples from the Jordan river water, inflows and groundwater in the vicinity of the lower Jordan valley, between the Sea of Galilee and Dead Sea.

ID	Loc.	Name	Distance from Alumot km	Date	$\delta^{11}B$ ‰	$^{87}Sr/^{86}Sr$	$\delta^{34}S_{sulfate}$ ‰	$\delta^{15}N_{nitrate}$ ‰	$\delta^{18}O_{water}$ ‰	TDS mg/l	Ca mM	Mg mM	Na mM	K mM	Cl mM	SO_4 mM	HCO_3 mM	NO_3 μM	Br μM	B μM	Sr μM
		Northern section																				
		Initial sources																				
JR-008	1	Sea of Galilee	0.0	01/09/99	25.5	0.70749	11.6			662	1.1	1.4	6.0	0.2	7.3	0.6	2.0	5	23	12	8
JR-107	2	Saline water carrier	0.0	25/9/00	32.0	0.70774			−4.4	4144	9.9	4.2	40.7	1.1	61.1	1.7	4.9	100	363	59	94
JR-225	3	Bitaniya	0	22/4/01				2.2	4.6	1811	1.4	3.7	12.0	2.3	13.4	0.9	12.0	16	30	28	10
JR-187	9	Fresh Yarmouk 1	2.6	04/12/01	31.5	0.70752				779	2.0	1.5	4.2	0.2	4.1	1.0	5.0	189	13	14	14
JR-368		Fresh Yarmouk 1	2.6	01/03/02	31.8	0.70754	10.6	11.7		735	1.9	1.3	3.9	0.2	3.4	0.8	5.3	161	13	12	11
JR-359	10	Fresh Yarmouk 2	3.3	01/03/02	32.8	0.70758	10.2	11.4		733	1.9	1.4	4.1	0.2	3.8	0.8	4.9	145	13	16	11
		River																			
JR-007	4	Alumot Bridge	0.1	01/09/99	29.2	0.70775	19.6			4673	10.6	4.9	47.8	1.6	68.4	1.8	5.6	16	313	55	99
JR-92		Alumot Bridge	0.1	08/08/00	32.8	0.70779	20.0			4264	9.8	4.4	43.0	1.2	62.4	1.8	5.1	16	375	45	89
JR-91	8	Dalhamiya Bridge	5.6	08/08/00	31.6	0.70773	13.5		−4.2	4007	8.9	4.5	38.5	1.2	57.5	2.3	5.3	32	338	55	78
JR-89	12	Gesher	8.7	08/08/00	33.5	0.70773	11.7		−3.6	4443	9.1	5.2	42.2	1.3	64.9	2.8	5.4	113	350	65	83
JR-94	13	Neve ur-North	11.6	08/08/00	34.8	0.70764	4.3		−2.7	4443	8.4	6.9	42.6	1.2	59.0	4.9	5.2	113	325	83	75
JR-96	15	Neve ur-South	12.7	08/08/00	32.3	0.70762	4.9	15.5	−3.3	3760	7.4	6.0	34.4	1.1	48.0	3.9	6.3	194	275	74	62
JR-004	26	Shifa' Station	28	10/01/03	31.5	0.70771	3.8			3523	4.9	7.5	33.5	0.9	44.3	4.3	5.5	177	143	65	40
JR-84		Shifa' Station	27.7	08/08/00	33.8	0.70770	5.9	16.1	−2.4	3761	6.2	7.0	35.2	0.9	47.1	3.9	7.0	161	200	65	49
		Eastern inflows and groundwater																			
JR-005	11	Yarmuok River	6.3	09/01/99	36.2	0.70719	−2.1			3245	3.6	8.1	27.4	0.8	29.4	7.5	7.4	258	106	176	24
JR-67		Yarmuok River	6.3	24/5/00	36.7	0.70716			−3.3	3371	3.6	8.5	30.5	0.7	31.9	7.4	7.1	161	125	205	24
1I	14	Wadi Arab	12.2	19/09/00	25.7	0.70784				678	1.6	1.5	4.2	0.2	4.9	1.1	3.2	110	8	20	10
1A		Wadi Arab	12.2	27/2/01	18.7	0.70775	−3.9			1599	3.3	3.8	11.4	1.2	8.5	5.3		4097	13		13
2B	16	Wadi Teibeh	16.5	04/01/01	21.0	0.70790	−5.4			3583	7.6	10.0	18.4	1.4	15.6	16.5	6.2	677	33	120	106
3A	17	Waqqas	17.6	27/2/01	29.8	0.70793				1074	1.8	4.7	8.7	0.2	6.9	4.2		548	13	48	27
4A	25	Abu Ziad	23.4	27/2/01	28.8	0.70870				406	1.4	1.9	3.2	0.2	3.3	1.0		73	5	13	11
		Western inflows and groundwater																			
JR-60	22	Harod	20.8	24/5/00	39.5	0.70782			−2.9	3914	5.4	6.1	39.4	0.7	55.3	2.1	7.3	32	100	40	28
JR-59	23	Water canal 48	21.4	24/5/00	38.2	0.70792			−4.6	4864	7.2	10.1	47.8	0.7	68.4	3.4	7.0	113	213	46	55
JR-58	24	Wadi Nimrod	22.2	24/5/00	38.0	0.70791			−3.8	3903	6.4	9.7	35.0	0.5	54.4	2.5	6.0	613	163	28	43
JR-61	18	Hamadia-well	18.2	24/5/00	31.7	0.70741			−1.4	3650	5.0	8.0	33.2	0.8	42.3	5.7	6.5	8	200	80	42
JR-73	20	En Huga	20.4	24/5/00	43.2	0.70783			−3.0	3241	6.1	6.2	28.8	0.5	44.0	2.4	5.6	355	113	31	32
JR-72	21	Hasida Spring	20.9	24/5/00	41.2	0.70780			−3.3	3349	6.3	6.9	29.7	0.7	46.1	2.2	5.6	371	138	32	31
JR-55		A-tin Spring	31.8	24/5/00	34.2	0.70794			−1.8	3845	5.5	11.1	32.5	0.5	53.3	2.8	6.8	48	175	49	54
		Central section																			
		Drainage																			
JR-189	5	Degania b	1.0	04/12/01	26.5	0.70755				4027	9.1	8.5	27.0	1.4	32.4	10.5	8.0	2065	128	148	26
JR-197	6	Afikim-groundwater	2.2	04/12/01	22.7	0.70760				3251	4.5	8.1	25.0	1.6	23.1	9.2	7.2	1323	103	167	24
JR-354	7	Kochvani h 1	2.2	01/03/02	27.1	0.70754		73		1632	2.3	2.8	14.3	0.9	18.2	1.7	4.8	16	38	33	13
		Fish ponds																			
JR-86	19	Hamadia-Eden	20.7	08/08/00	31.5	0.70762			0.4	4436	6.6	8.3	42.6	1.4	57.3	6.4	4.3	161	300	111	64
		River																			
JR-50	28	Gibton	44	24/5/00	36.71	0.70785			−3.3	2983	3.4	7.1	28.6	0.7	38.4	3.9	4.1	48	114	76	35
		Eastern inflows and groundwater																			
10	29	Rajib Seebiya	49	19/09/00	26.97	0.70804				1862	3.2	5.1	13.3	0.6	16.8	3.1	5.1	1160	102	119	79
8	30	Bassat Faleh	51	18/09/00	30.22	0.70806				1883	3.1	4.9	12.6	0.6	10.4	4.6	6.1	2280	54	76	29
9	31	Faleh Botton	51	18/09/00	40.46	0.70809				2982	6.3	7.6	19.9	1.0	30.6	5.2	6.7	700	267	71	28
7	32	Bweib	53	18/09/00	29.22	0.70797				1962	4.1	5.1	12.6	0.7	10.4	6.2	4.7	1640	64	70	25
12	33	Wadi Mikman	55	18/09/00	26.22	0.70804				3847	7.2	10.5	23.8	1.5	23.2	14.0	6.1	2440	64	167	112
13	34	Hawwaya	57	18/09/00	19.73	0.7082				5900	15.4	14.9	25.5	4.1	29.7	26.8	7.1	1790	38	246	161
14	35	Mifshel	59	18/09/00	28.97	0.70827				5038	8.7	13.9	30.3	4.4	28.1	22.3	3.7	2000	24	77	18
		Western inflows and groundwater																			
JR-014	27	Wadi El-maliach	38	09/11/99			22.2		−4.1	3123	6.4	4.4	29.4	1.1	42.3	3.5	3.0	121	232	65	65
JR-51		Wadi El-maliach	38	23/5/00	37.96	0.70776			−4.6	3033	6.2	4.8	27.5	0.9	37.7	3.5	4.7	323	188	81	59
JR-247		Wadi El-maliach	38	06/04/01						3199	6.9	5.3	28.9	1.0	39.4	3.8	5.0	281	163	56	60
		Southern section																			
		River																			
JR-81	36	Zarzir Station	59.7	08/07/00	32.6	0.70797	6.3	16.4	−2.2	3458	4.2	7.9	32.6	1.2	41.5	5.4	4.7	177	150	92	46
JR-103		Zarzir Station	59.7	25/9/00	32.5	0.70788		13.7	−2.2	3459	5.1	7.5	31.5	1.0	41.6	4.6	6.0	295	135	74	46
JR-80	38	Damya (Adam) Bridge	66.4	08/07/00	30.7	0.70810	7.2	16.7	−3.2	3617	4.5	7.9	34.4	1.4	42.3	6.1	4.7	226	138	102	51
JR-102		Damya (Adam) Bridge	66.4	25/9/00	30.5	0.70806		14.3	−2.1	3409	5.3	7.4	31.8	1.1	41.2	5.2	4.1	332	131	79	51
JR-233		Damya (Adam) Bridge	66.4	23/4/01						4782	7.0	10.9	43.5	1.7	54.0	8.3	6.9	394	212	129	68
JR-100	44	Tovlan Station	72.4	25/9/00	30.0	0.70805		14.4	−1.7	3881	5.8	8.2	35.2	1.3	45.7	6.2	0.4	365	150	111	56
JR-126		Tovlan Station	72.4	27/2/01	32.0	0.70804			−3.7	3902	6.1	8.4	35.1	1.3	43.1	6.5	0.6	565	200	106	68
JR-231		Tovlan Station	72.4	23/4/01					−3.1	5970	8.4	13.0	54.4	2.0	71.2	10.5	0.4	415	365	176	80
JR-45	47	Gilgal-107	76.6	23/5/00	33.0	0.70814		14.5	−2.8	5406	6.4	12.3	51.1	1.9	65.1	10.1	4.6	371	263	176	79
JR-78		Gilgal-107	76.6	08/07/00			7.1	15.75	1.9	4350	5.2	9.3	40.7	1.6	52.8	7.7	4.4	306	250	139	59
JR-230		Gilgal-107	76.6	23/4/01					−3.4	6120	8.6	13.8	56.1	2.0	75.0	10.2	6.3	397	308	171	82
JR-002	49	Allenby Bridge	91.4	09/01/99	30.7	0.70820	5.8			4851	5.6	10.6	46.1	2.0	57.5	9.4	4.0	484	185	176	71
JR-7b		Allenby Bridge	91.4	08/07/00	31.7	0.70807	5.0	16.2	−2.4	4724	5.6	10.4	48.7	2.0	55.8	8.1	4.1	274	288	166	
JR-332		Allenby Bridge	91.4	08/12/01					−2.9	7866	9.2	17.7	73.9	3.4	97.8	15.2	3.9	403	563	231	108
JR-001	50	Baptism site	95.6	09/01/99	31.0	0.70813	5.7			4886	5.6	10.7	45.7	2.0	58.8	9.4	4.0	477	202	166	73
JR-75		Baptism site	95.6	08/07/00	31.6	0.70816	6.4	16.8	−4.7	5063	5.9	11.3	47.8	2.1	62.1	9.1	4.1	274	363	176	74
JR-331		Baptism site	95.6	08/12/01					−2.3	10278	12.5	24.4	97.9	4.2	131.8	18.3	4.0	484	826	268	153
JR-74	54	Abdalla Bridge	100.0	08/07/00			7.3	17.13	−2.9	6218	7.0	14.6	57.9	2.6	79.0	10.8	4.2	306	401	213	90
JR-99		Abdalla Bridge	100.0	25/9/00	30.2	0.70805		14.8	−1.6	4469	6.5	9.6	40.7	1.5	54.4	7.2	5.2	379	253	129	67
JR-330		Abdalla Bridge	100.0	08/12/01					−2.4	11095	13.6	29.0	100.0	4.3	151.5	17.2	4.2	333	1014	259	159

Table 1. (Continued)

ID	Loc.	Name	Distance from Alumot km	Date	$\delta^{11}B$ ‰	$^{87}Sr/^{86}Sr$	$\delta^{34}S_{sulfate}$ ‰	$\delta^{15}N_{nitrate}$ ‰	$\delta^{18}O_{water}$ ‰	TDS mg/l	Ca mM	Mg mM	Na mM	K mM	Cl mM	SO_4 mM	HCO_3 mM	NO_3 μM	Br μM	B μM	Sr μM
		Eastern inflows and groundwater																			
6	37	Zarqa River	66.3	18/09/00	24.7	0.70871				4245	8.8	9.0	30.8	1.7	38.3	11.6	5.8	1010	131	210	88
18A		Zarqa River	66.3	27/2/01	24.2	0.70868	9.5			4518	6.0	8.6	45.7	2.6	48.2	12.0	0.0	790	116	235	94
17B		Zarqa River	66.3	04/01/01	27.5	0.70857	10.0			4796	6.3	8.5	46.5	2.7	48.5	11.9	4.8	16	113	191	96
4	40	Rasif	69.2	18/09/00	33.7	0.70836				12450	11.3	30.8	118.7	3.4	136.4	31.6	5.1	1810	1098	748	146
5	41	Abu Mayyala	70.3	18/09/00	28.7	0.70822				11360	8.2	12.7	137.0	3.9	122.9	26.0	6.4	2040	675	691	170
24A	42	Aqraa	70.3	27/2/01	48.2	0.70802				71034	59.2	188.8	726.4	27.0	1170.6	43.6	0.0	1355	6821	1908	516
16B		Aqraa	70.3	04/01/01	48.6	0.70794	10.2			68497	49.2	185.1	739.5	29.4	1078.3	43.1	4.4	8065	9262	1916	491
15	43	Mallaha Gdeida	70.4	18/09/00	28.5	0.70807				3811	7.7	10.3	22.0	2.6	27.2	13.5	6.1	90	98	1069	161
25A	45	Mallaha	72.5	27/2/01	29.5	0.70810	5.6			15508	18.5	25.0	167.5	7.8	166.4	40.9	0.0	2225	451	1227	171
2	51	Kharar	96.8	13/09/00	29.0	0.70805				5741	11.3	9.2	48.6	3.4	62.2	9.2	11.3	220	230	147	236
1	52	Hisban Kafrain	98.8	13/09/00	40.2	0.70816					11.8	9.8	47.4	4.0	65.9	8.6	10.0	990	322	76	113
		Western inflows and groundwater																			
JR-48	39	Tirtcha Upper	66.7	23/5/00	40.2	0.70800			−4.3	7386	8.5	19.5	54.7	2.2	75.5	14.0	19.2	258	300	217	106
JR-46	46	Wadi el Ah'mar	75.0	23/5/00	41.7	0.70796	4.3		−3.0	62911	88.1	163.6	601.2	29.0	1069.0	18.8	1.8	2	7885	430	793
JR-43	48	Uga Melccha	86.7	23/5/00	41.7	0.70797			4.7	5274	7.5	13.5	42.8	2.3	63.5	9.7	5.4	500	388	231	66
JR-77		Uga Melecha	86.7	08/07/00			−17.1	11.11	−6.2	5251	7.5	14.1	44.6	2.6	63.5	9.3	5.1	484	44	241	66
JR-333		Uga Melecha	86.7	08/12/01	41.5	0.70804	−16.7			5391	7.6	14.4	43.5	2.6	65.9	9.6	5.2	403	451	185	65
JR-13		Sukot Spring	37.4	29/3/00	47.5				−4.8	1648	3.7	3.7	10.0	0.1	12.6	1.9	7.4	1619	36	25	14
JR-52		Sukot Spring	37.4	23/5/00		0.70798		4.54	−4.8	1632	3.7	3.6	10.4	0.1	12.1	1.8	7.4	1613	38	31	13
JR-41	53	Hagla-well	96.7	23/5/00	43.5	0.70799			−5.0	2333	5.9	7.2	12.5	1.3	26.8	3.5	4.1	661	63	63	110

The content of individual constituents are reported in mM, where the overall total dissolved salts (TDS) values are in mg/l. Location of the sampling sites are marked in Figure 1. Distance (in km) refers to the initial flow of the Jordan River at Alumot Dam.

a solute mass balance (Table 3) we found that the initial flow consists of 60 to 90% of the saline water carrier. The chemical and isotopic compositions of the base flow Jordan River water (e.g., Na/Cl~ 0.65, SO_4/Cl~0.03; $\delta^{34}S_{sulfate}$=20‰; Table 2) maintain the Ca-chloride (i.e., Ca/(HCO_3+SO_4) >1) fingerprint of the saline springs that emerge at the western shore of the Sea of Galilee (Starinsky, 1974; Kolodny et al., 1999) and are diverted through the saline water carrier to the Lower Jordan River.

The initial chemical and isotopic composition of Jordan River water at Alumot dam is significantly modified downstream, particularly along the upper 12 km (Figs. 3 and 4). We observed a decrease in Cl^-, Br^-, Na^+, K^+, Ca^{2+}, Sr^{2+}, $\delta^{34}S_{sulfate}$, and in $^{87}Sr/^{86}Sr$ ratio and an increase in Mg^{2+}, SO_4^{2-}, B, $\delta^{15}N_{nitrate}$ and $\delta^{18}O_{water}$ values (Table 2 and Figs. 4, 5 and 6). The $\delta^{34}S_{sulfate}$ values decrease from 20‰ to 5‰, $^{87}Sr/^{86}Sr$ ratios decrease from 0.70779 to 0.70760, $\delta^{18}O_{water}$ increases from ~-4.5‰ to −2‰, and boron isotopes show no systematic variation ($\delta^{11}B$ between 29–35‰ (Figs. 6 and 7)) despite a significant increase in the boron content (Table 2). Overall, the Ca-chloride composition (i.e., Ca/(SO_4+HCO_3)>1) of the initial saline water is modified into a Mg-chloride water type and the Na/Cl and SO_4/Cl ratios increase downstream. Figure 5 shows that the contents of differ-

Table 2. Major water resources in the vicinity of the Jordan valley that flow or are associated with the Jordan River.

Water source	TDS* (g/l)	Geochemistry	Sample (see Table 1)
Initial river			
Saline springs that emerge at the western shore of the Sea of Galilee composed of the "Saline Water Carrier"	4.1 to 5.2	Ca-Chloride type with low Na/CI and SO_4/CI ratios	2
Bitania sewage effluents	1.7 to 1.8	High Na/CI low SO_4/CI	3
Northern section			
Agricultural return flows mixed with natural saline groundwater	1.4 to 8.6	Mg-Chloride type enriched insulfate with high Na/CI and SO_4/CI ratios; high nitrate	5; 6; 7; 11; 18
Eastern inflow and groundwater	0.6 to 3.7	Na-Chloride type extremely enriched in sulfate with high Na/CI and SO_4/CI ratios	14; 16; 17; 25
Saline western inflows and groundwater	3.2 to 4.9	Ca-Chloride type with low Na/CI and SO_4/CI	20; 21; 22; 23; 24
Central section			
Eastern agricultural return flows	0.5 to 5.9	Mg-Chloride type extremely enriched in sulfate with high Na/CI and SO_4/CI ratios	29; 30; 31; 32; 33; 34; 35
Western saline springs (Wadi El-Maliach)	2.9 to 3.2	Ca-Chloride type with low Na/CI and SO_4/CI ratios	27
Southern section			
Zarqa saline springs that emerge from the Jurassic and Lower Cretaceous rocks	4.2 to 16.0	Mg-Chloride with high Na/CI and SO_4/CI ratios	37; 40; 41
Shallow springs and groundwater emerge from the Pleistocene sediments	2.5 to 15.5	Mg-Chloride enriched in sulfate with high Na/CI and SO_4/CI ratios, high nitrate	39; 43; 45; 48; 51; 52
Hypersaline brines	60.0 to 80.6	Ca-Chloride with low Na/CI and SO_4/CI ratios	42; 46 (53)

For full information see Table 1.
* Total dissolved salts.

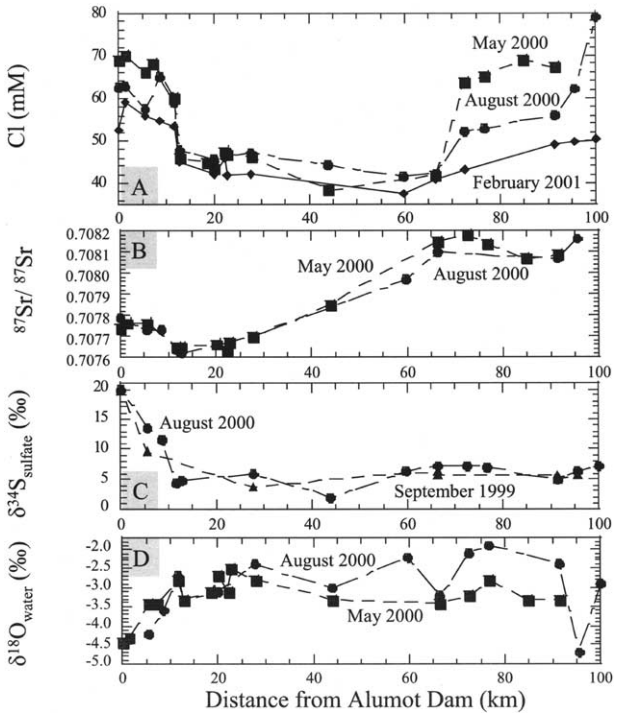

Fig. 3. Chloride (mg/L), strontium, sulfur, and oxygen isotopic variation transects along the Jordan River. See Table 2 for the complete isotopic data.

ent ions tend to correlate linearly with chloride along the river flow. These relationships indicate that the chemical modification of the Jordan River water is mainly controlled by mixing of the initial river water with a second water type that has a distinct chemical composition (i.e., Fig. 6). This water source also has low $\delta^{34}S$ and $^{87}Sr/^{86}Sr$ values and high $\delta^{15}N_{nitrate}$ and $\delta^{18}O_{water}$ values relative to the initial river water at Alumot Dam.

Table 4 summarizes and Figure 6 illustrates the geochemical characteristics of the known tributaries and groundwater in the upper part of the Jordan River: the eastern tributaries (from Jordan), the western tributaries (from Israel), the saline Yarmouk River, and shallow drainage waters that were collected from shallow boreholes in the vicinity of the Yarmouk River (Fig. 2). The chemical and isotopic compositions of the eastern and western tributaries cannot account for the observations within the river (Table 4). For example, the western inflows have higher $^{87}Sr/^{86}Sr$ and lower SO_4/Cl ratios than the river water and are therefore not consistent with the trend observed in the river (Fig. 6). Also the eastern inflow has a high $^{87}Sr/^{86}Sr$ ratio.

In contrast, the chemical and isotopic variations recorded in the Jordan River are similar to that of the saline Yarmouk River and its shallow drainage waters (e.g., high Na/Cl and SO_4/Cl, and low $\delta^{34}S_{sulfate}$ and $^{87}Sr/^{86}Sr$ values (Figs. 6 and 7)). Most of the freshwater of the Yarmouk River (TDS~730 mg/L; Table 2) is diverted to King Abdalla Canal, about eight km upstream from its confluence with the Jordan River. However, we found that the Yarmouk River water downstream from the diversion is saline (TDS~2800 to 8600 mg/L) with a distinct chemical and isotopic composition (Table 2). This composition (Na/Cl=0.78 to 0.96; SO_4/Cl=0.2 to 0.3; $^{87}Sr/^{86}Sr$ ~0.70717; $\delta^{34}S_{sulfate}$ = −2.1‰) is identical to that of a postulated end member that controls the chemical and isotopic changes observed in the northern section of the Jordan River (Table 4 and Figs. 6 and 7). Hence a common groundwater source controls the water quality of both the northern Jordan River and the saline Yarmouk River. Since the chemical and isotopic modifications of the Jordan River water along the upper 12 km are gradual (Figs. 3, 4 and 5), and are not restricted to the area below the confluence of the saline Yarmouk River at 6 km downstream (Fig. 2), we propose that diffuse groundwater discharge is particularly effective along this section of the river. In fact, the water of the saline Yarmouk River is pumped out for fishpond recharge before the confluence with the Jordan River and hence its direct contribution is negligible.

In addition to the gradual changes, the concentrations of most ions in the Jordan River sharply decrease after the confluence of Wadi Arab, ~12 km downstream from Alumot dam (Fig. 4). However, the water composition of Wadi Arab cannot explain the chemical and isotopic variations of the Jordan River water at this point (e.g., relatively high $^{87}Sr/^{86}Sr$ ratios of 0.70775 to 0.70784; Table 2). We argue that relatively high

Table 3. Calculations of the mixing proportions between saline diverted water ("saline carrier") and sewage effluents ("Bitaniya") that compose the initial base flow of the Jordan River at Alumot bridge.

ID	name	Date	Ca (mM)	*f* (%)	Mg (mM)	*f* (%)	Na (mM)	*f* (%)	CI (mM)	*f* (%)	SO_4 (mM)
JR-119	Saline Water Carrier	12-2000	12.34	78	5.19	77	51.55	79	78.27	76	1.92
JR-118	Bitania		2.52	22	2.22	23	11.79	21	12.13	24	1.03
JR-117	Alumot Bridge		10.22	100	4.50	100	43.13	100	62.56	100	1.72
JR-149	Saline carrier	02-2001	12.74	60	5.23	61	51.11	64	77.99	61	1.88
JR-148	Bitania		2.55	40	2.18	39	11.4	36	12.47	39	1.00
JR-147	Alumot Bridge		8.67	100	4.03	100	36.97	100	52.46	100	1.56
JR-179	Saline carrier	03-2001	9.64	90	4.28	86	40.89	87	62.34	86	1.72
JR-180	Bitania		2.62	10	2.22	14	11.48	13	12.47	14	0.99
JR-178	Alumot Bridge		8.97	100	3.99	100	37.19	100	55.57	100	1.55
JR-224	Saline carrier	04-2001	10.84	85	4.69	61	46.11	83	67.55	83	1.80
JR-225	Bitania		1.44	15	3.74	39	11.96	17	13.37	17	0.92
JR-223	Alumot Bridge		9.44	100	4.32	100	40.45	100	58.39	100	1.67

Calculations were made for different major elements.

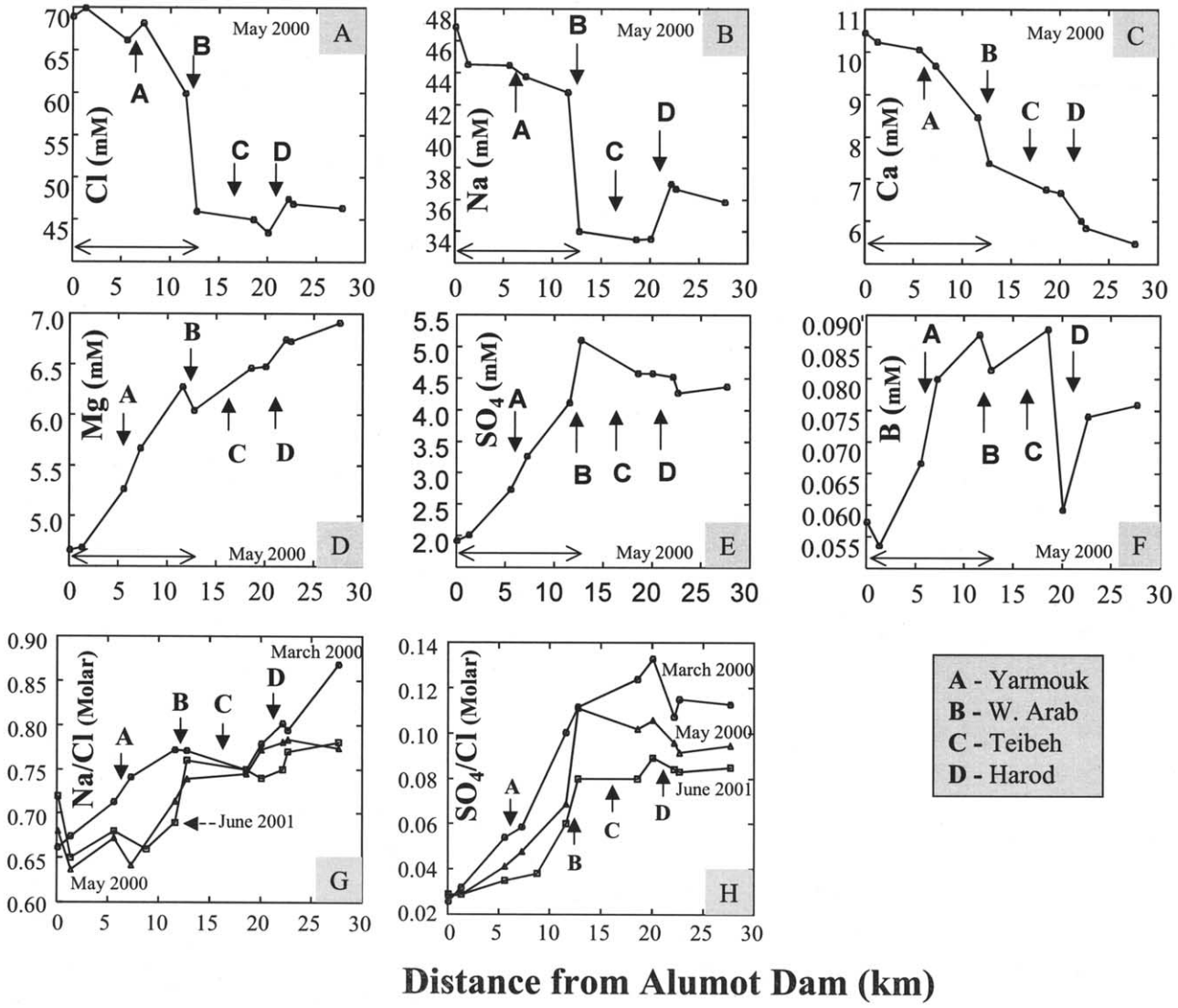

Fig. 4. Major ions, Na/Cl and SO_4/Cl ratios transects along the northern Jordan River sampled in May 2000. Note the gradual variations of Mg^{2+}, SO_4^{2-}, B, Na/Cl, and SO_4/Cl, and the sharp decrease of Cl^- and Na^+ after the confluence of Wadi Arab. Arrows mark the other major tributaries.

inflow of Wadi Arab (Holtzman, 2003) that is characterized by low dissolved solid contents (chloride range of 4.8 to 8.8 mM; Table 2) causes a point dilution of the downstream Jordan River water. Nevertheless, the overall chemical modification of the Jordan River is dominated by the groundwater discharge with a significantly lower $^{87}Sr/^{86}Sr$ ratio. In sum, our results confirm hypothesis #3 that both the Yarmouk and Jordan rivers are influenced by discharge of a common (non-point) groundwater source. From 12 km downstream the groundwater discharge is superimposed with a point surface inflow of Wadi Arab (i.e., hypothesis #2).

Using mixing equations we determined the relative proportion of the groundwater component in the northern Jordan River. The equations assume that the concentration *C(x)* of conservative species in the river is determined by mixing with the groundwater component as follows,

$$C(x) = C_Y f(x) + C_i(1 - f(x)) \quad (1)$$

C_i is the initial river concentration (at Alumot), C_Y is the concentration in the saline Yarmouk River (which is considered to be a good proxy for the groundwater composition) and *f* is the groundwater component discharge divided by the total river discharge. We have calculated *f* values for each of the sampling months. Correlating *f* with distance from the river source (Alumot) was obtained by applying Equation 1 using chloride concentration. Computed concentrations of sodium, sulfate and other species were then calculated as a function of *f*. Theoretical curves of ion ratio versus chloride concentration were finally plotted and compared with measured values. Figure 8 illustrates an example for Na/Cl, SO_4/Cl, and Mg/Cl variations in the Jordan River during December 2000. The variations of these ionic ratios determined for Jordan River water along the upper 12 km follow the theoretical mixing line between the

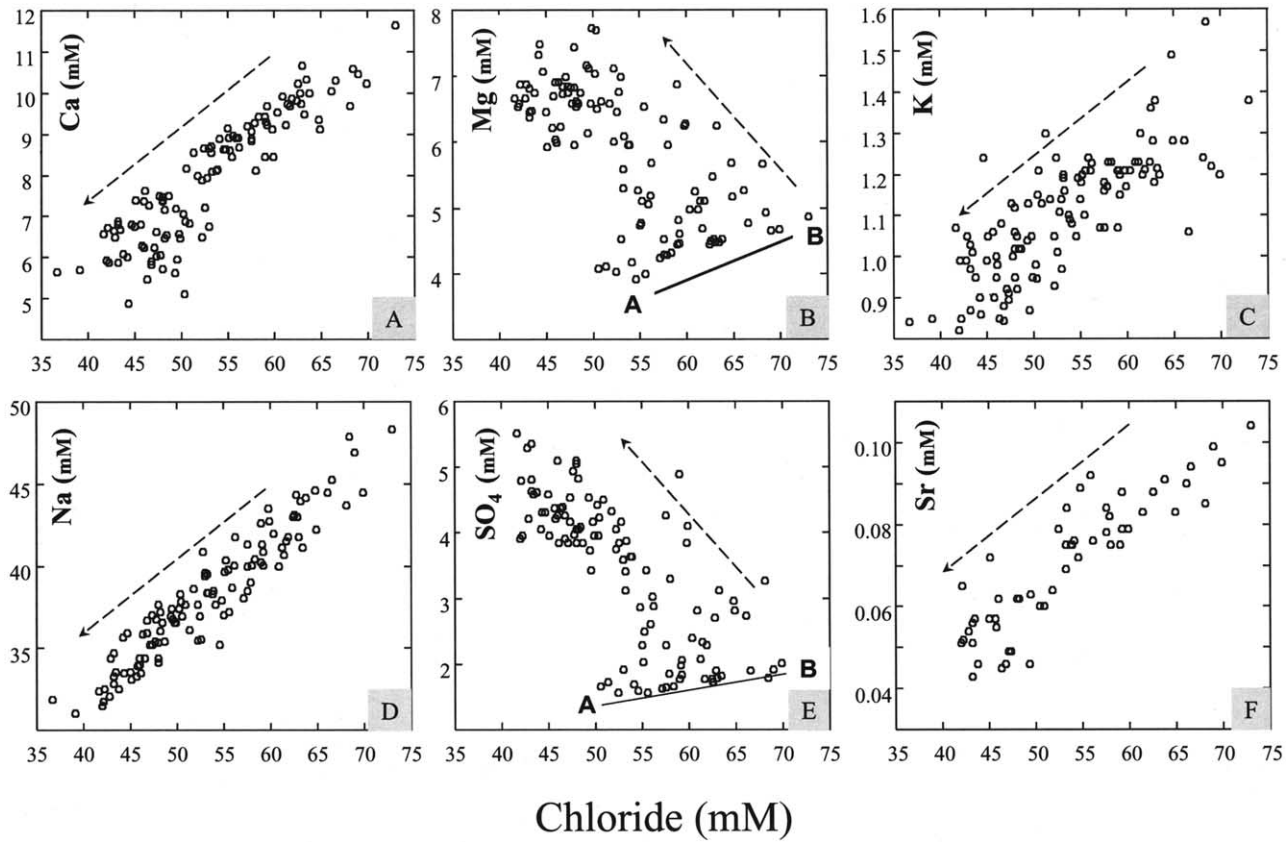

Fig. 5. Major elements versus chloride content in the northern section of the Jordan River. Arrow represents the river flow direction. Line A-B (graphs B and E) represents a mixture between sewage effluents and saline diversion water, which compose the base flow of the lower Jordan River at Alumot Dam.

initial river water and the saline Yarmouk River. We found that the different ionic ratios yield similar results and determined that the overall contribution of the groundwater discharge varies between 20 and 50% of the total river flow (measured at ~12 km downstream from Alumot). In a parallel study we have applied flow rate measurements and detailed water mass-balance calculations along small segments of the river (Shavit et al., 2002; Holtzman et al., 2003). The flow rate values obtained in the northern part of Jordan River vary from 600 to 900 L/s. Thus our mixing calculations of groundwater discharge of 20 to 50% of the river flow infer a contribution of 120 to 450 L/s to the river.

4.2. The Origin of the Shallow Groundwater in the Northern Section of the Lower Jordan Valley

We sampled shallow groundwater and drainage water from several piezometers in the northern Lower Jordan Valley (Fig. 2 and Tables 1 and 2). The shallow drainage water represents local agricultural return flow that flows to the Jordan and Yarmouk Rivers. Figure 6D shows that the saline Yarmouk water and the shallow drainage water have a similar chemical composition. The apparent chemical similarity of both water sources suggests that the shallow groundwater that flows into the Yarmouk and Jordan rivers is derived primarily from agricultural return flows. This conclusion is also consistent with the relatively high $\delta^{18}O_{water}$ values (Fig. 6) and relatively high nitrate levels with elevated $\delta^{15}N$ values observed in the saline Yarmouk River (30 mg/L) and drainage water (140 mg/L), as well as the net addition of nitrate to the northern section of the Lower Jordan as was reported by Segal et al. (2004).

The chemical and isotopic compositions of the saline Yarmouk River are not identical to that of the fresh Yarmouk River and Sea of Galilee, which are the major sources of irrigation water in the Northern Jordan Valley. For example, the fresh water resources have high $\delta^{34}S_{sulfate}$ values (10.6‰ and 11.6‰ in the Sea of Galilee and fresh Yarmouk River, respectively) relative to the saline Yarmouk with a low $\delta^{34}S_{sulfate}$ value (−2.1‰; Table 2). In addition, the low $^{87}Sr/^{86}Sr$ ratio in the saline Yarmouk (~0.70718) is not consistent with that of the western inflows (0.7079 to 0.7082), eastern inflow (0.70775 to 0.7087), the fresh Yarmouk River (0.70754), and the Sea of Galilee (0.70749). The inconsistency between the compositions of the fresh irrigation waters and the agricultural return flows can be due to two possible explanations; a modification of the irrigation waters by addition of fertilizers, or a mixing with external water sources.

Böhlke and Horan (2000) have shown that fertilizers and hence agricultural recharge may have $^{87}Sr/^{86}Sr$ signatures distinctive from those of natural water-rock interactions. Alternatively, if the change comes about by mixing with an external

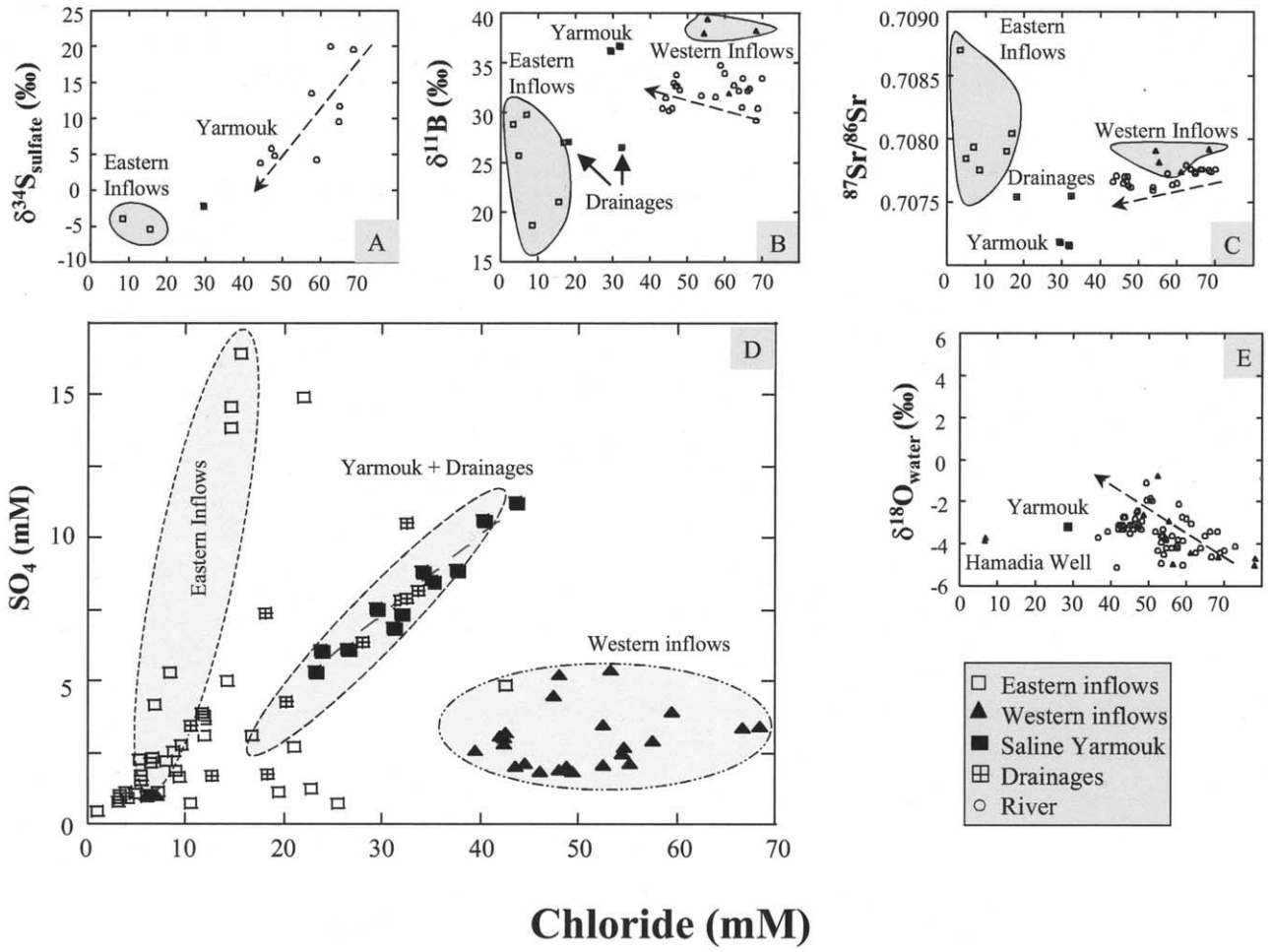

Fig. 6. $\delta^{34}S_{sulfate}$, $^{87}Sr/^{86}Sr$, $\delta^{18}O_{water}$, $\delta^{11}B$ values and sulfate concentration versus chloride content in the northern Jordan River (open circles), eastern inflows, western inflows, saline Yarmouk River, and drainage water. Hamadia well collects shallow groundwater underlying fishponds and represents drainage of $\delta^{18}O_{water}$ enriched effluents of overlying fishponds. Arrow represents the river flow direction.

water source, such a source could not have been formed exclusively by evapotranspiration of irrigation water. This source could be represented by the eastern tributaries that have typical high SO_4/Cl and low $\delta^{34}S_{sulfate}$ values (e.g., Teibeh, $\delta^{34}S_{sulfate} = -5.4$‰), and an unrecognized groundwater component, characterized by a low $^{87}Sr/^{86}Sr$ ratio. The low $^{87}Sr/^{86}Sr$ ratio is associated also with a high Mg/Ca ratio (2–3; Table 2), which indicates the basaltic rocks influence on groundwater composition (e.g., Hem, 1985). The major two basaltic aquifers in the northern Jordan valley are those of the Yarmouk basin in the east and the basaltic aquifer in the west (Fig. 1; Rosenthal, 1987; Möller et al., 2003). Furthermore, the composition of the shallow groundwater can be shaped by interaction with basaltic gravels within the Jordan Valley, particularly in areas in the vicinity of side wadis and paleo channels.

In summary, the inferred groundwater discharge to the Jordan and Yarmouk rivers has unique chemical and isotopic compositions; high Na/Cl, Mg/Ca, SO_4/Cl, and B/Cl ratios and low $\delta^{34}S_{sulfate}$ and $^{87}Sr/^{86}Sr$ values (Table 2 and Fig. 6). High concentrations of nitrate and elevated $\delta^{15}N$ values as well as high $\delta^{18}O_{water}$ values indicate a significant contribution from

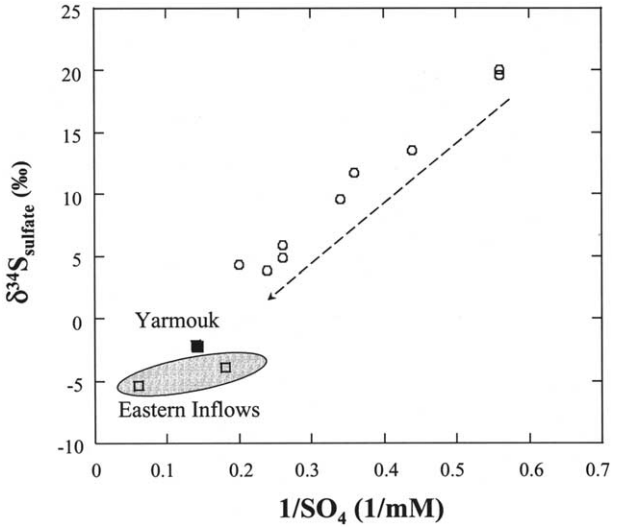

Fig. 7. $\delta^{34}S_{sulfate}$ values versus reciprocal of sulfate of the northern Jordan River (open circles), saline Yarmouk, and eastern inflows.

Table 4. A summary of the major geochemical features (isotopic compositions and ionic ratios) that characterize the major sources in the northern section of the Lower Jordan valley.

	Calculate end-member	Saline Yarmouk	Eastern inflows	W. Teibeh	Fish ponds	Western inflows
CI (mM)	<34	23–45	<20	15–21	45–71	28–71
SO_4 (mM)	>5.5	5.5–11	0.5–5.5	14–17	2.5–6.5	2–13
Na (mM)	<30	22–37	1–11	17–18	30–49	28–49
Mg (mM)	>6	6–12.5	1–4.5	9–12.5	6.5–10	5–12
Ca (mM)	<5	3.5–5	1.5–4	6–8.5	3.5–8.5	5–8.5
Na/Cl	>0.8	0.85–0.95	1	0.8–1.2	0.62–0.77	0.68–0.75
SO_4/CI	>0.12	0.23–0.26	0.2–0.3	1	0.05–0.11	0.05–0.07
$^{87}Sr/^{86}Sr$	<0.7075	0.7072	0.7076–0.7087	0.7079	0.70762	0.70741–0.70791
$\delta^{11}B$	28–36‰	36‰	28‰	21‰	31.5‰	22–43‰
$\delta^{34}S$	<5‰	(−2)‰	(−4)−(−5)‰	(−5.4)‰	No data	No data

The different geochemical parameters are compared with postulated "end member" that directly controls the Jordan River water. The white background represents a geochemical parameter that is consistent with that observed along the northern section of the Jordan River. The gray background represents a geochemical parameter that is not consistent with that observed along the northern section of the Jordan River.

agricultural return flows. The high sulfate concentrations can be derived from weathering of fine grained sediments from the Lisan and Samra formations. Hem (1985) showed that weathering of exposed fine grained sediments in the Western United States combined with capillary evaporation to the surface, result in sulfate enrichment that was recorded in the Moreau and Rio Grande summer flows. The low $\delta^{34}S_{sulfate}$ values (−2‰ in the saline Yarmouk River) suggest that the original source of sulfur in these sediments is probably pyrite or some other form of ferrous sulfide that was oxidized in the sediments. Hence, we propose that this inferred groundwater discharge is derived from multiple sources that include agricultural return flow, groundwater that has interacted with basaltic rocks (and hence derived from two possible basaltic aquifers in the region (Fig. 1)), and groundwater that has interacted with fine grained sediments depleted in ^{34}S either within the Jordan valley or from the eastern side of the Jordan Valley (Fig. 1).

4.3. Chemical Modification in the Central Section

In the central segment, 20 to 60 km downstream from Alumot Dam, the sampling points were limited due to logistic and security reasons. In addition, the monitoring sites for surface water inflows and groundwater at the two sides of the river are uneven with a large number of inflows on the eastern side and only a few in the western side (Table 2 and Fig. 2). In contrast to the northern and the southern sections, we observed only minor salt content variations in the Jordan River water despite a significant downstream increase of the $^{87}Sr/^{86}Sr$ and SO_4/Cl ratios (Fig. 3). The major western inflow in this area is Wadi el Maliach with chloride concentrations of 36−42 mM, $^{87}Sr/^{86}Sr$ of 0.70776, and SO_4/Cl ratios of 0.08−0.1. In contrast, the eastern inflows and groundwater have a chloride range of 2.8 to 48 mM, $^{87}Sr/^{86}Sr$ of 0.7080 to 0.7087, and SO_4/Cl ratios of 0.01 to 0.8 (Table 2). The increase of the $^{87}Sr/^{86}Sr$ and SO_4/Cl ratios observed in the river indicates that the eastern inflows have a major control on the chemical and isotopic compositions of the river water while the western inflow, with lower $^{87}Sr/^{86}Sr$ and SO_4/Cl ratios, is negligible. We suggest that the predominance of agricultural activity and the relative richness in water resource along the eastern side result in surface water flow and modification of the Jordan River along this segment.

4.4. Chemical Modification in the Southern Section

The southern section of the Jordan River (60 to 100 km from Alumot dam) is characterized by a downstream increase in the salt contents (Fig. 9). Overall, the contents of all of the dissolved solutes increase linearly with chloride (Fig. 10). We observed seasonal variations in the intensity and locations of chemical modifications accompanying this salt increase. During fall and winter, the salt content in the Jordan River rises gradually downstream, but its magnitude is small (a chloride increase of only 9 mM between Adam and Abdalla bridges (Fig. 2)). During the spring months, the Jordan River has a saline peak (TDS up to 6000 mg/L) at a distance of 70−80 km from Alumot dam. During the summer months the salt content increases continuously with distance (TDS of 11090 mg/L during August 2001) before the river enters the Dead Sea (Fig. 9A). The changes in the dissolved salt patterns are also associated with changes in chemical compositions. The Jordan River water at a distance of 60 to 90 km downstream from Alumot dam is characterized by Na/Cl>0.75, SO_4/Cl>0.145. Further south at a flow distance of >90 km, the rise of salt content is associated with Na/Cl<0.75, SO_4/Cl<0.145 (Fig. 11). In contrast to the large variations of the total dissolved salts, the isotopic values of $^{87}Sr/^{86}Sr$, $\delta^{34}S_{sulfate}$, $\delta^{18}O_{water}$ (Fig. 3) and $\delta^{15}N_{nitrate}$ (Table 2) vary only marginally in the lower part of the Jordan River, except for a slight increase of $^{87}Sr/^{86}Sr$ ratios at a flow distance of 65–75 km (i.e., Adam Bridge, $^{87}Sr/^{86}Sr$=0.70803 to 0.70815).

A detailed survey of all eastern and western wadis that flow to the Jordan River and groundwater in the vicinity of the southern Jordan Valley (Table 1) reveals that the inflows in the southern section include brackish water from the Zarqa River and two types of groundwater: one is a brine represented by Wadi Ah'mar (on the west) and Aqraa (on the east), having the typical Ca-chloride composition of the Dead Sea Rift valley (Starinsky, 1974; Stein et al., 1997), and the other is a sulfate-rich saline spring (e.g., Mallaha and Bassat El Faras on the eastern side) that represents groundwater (Table 2). The brackish water of the Zarqa River is derived from natural saline springs that emerge within the Jurassic and Lower Cretaceous rocks and is characterized by Na/Cl~0.9, SO_4/Cl~0.25, high $^{87}Sr/^{86}Sr$ (~0.7087), and relatively low $\delta^{11}B$ (~25‰; Fig. 12).

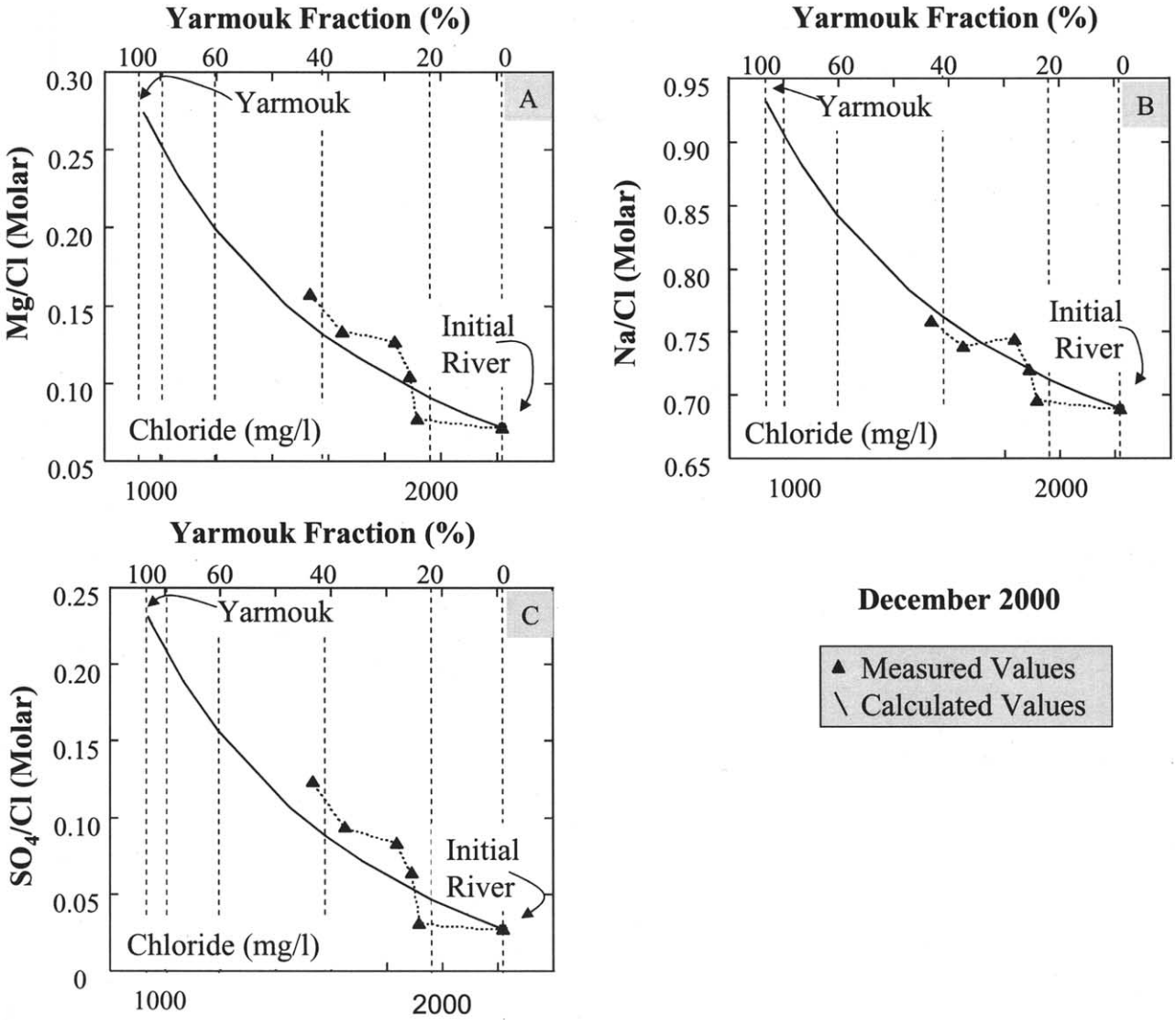

Fig. 8. Mg/Cl, Na/Cl and SO_4/Cl ratios versus chloride concentrations in the upper 12 km of the Jordan River sampled during December 2001. The measured data (black triangle) are compared to calculate mixing lines between the initial river at Alumot dam and the saline Yarmouk River as sampled in that month. Note the increasing fraction of the groundwater component, represented by the composition of the saline Yarmouk, along the flow of the Jordan River.

The brines have low Na/Cl (0.55–0.69) and SO_4/Cl (0.02–0.04), high Br/Cl (5–9 $\times$ 10^{-3}), and $\delta^{11}B$>40‰ (Table 2). In contrast, the sulfate-rich groundwater has high Na/Cl (0.8–1.0), SO_4/Cl (0.25–0.5), low Br/Cl ratios (1–4 $\times$ 10^{-3}), and $\delta^{11}B$ ~30‰. This type of saline groundwater was identified in the Jericho area near the southern end of the river (Marie and Vengosh, 2001). Both groundwater and brines have $^{87}Sr/^{86}Sr$ ratios of ~0.7081 and $\delta^{34}S_{sulfate}$ values of 4‰ to 10‰. (Table 1 and Fig. 12).

The variations in the content of dissolved salts, the chemical modification along the river, and specific chemical and Sr isotopic mass-balance calculations using water before and after the confluence of the Zarqa River to the Jordan River clearly indicate that the source of salts in the southern section of the river cannot be explained by a single surface inflow, or by net evaporation of the river along its flow. The latter is evidenced by the changes in the ionic ratios along the flow (Fig. 11) and the lack of significant increase of $\delta^{18}O_{water}$ values that would accompany a rise in salt content due to evaporation (Fig. 3). Figure 13 illustrates a linear correlation (R^2 = 0.912) between Cl^- and SO_4^{2-}, which indicates a single source of the dissolved salts. The composition of this source appears to be different, however, from those of the brines or sulfate-rich groundwater. Hence, none of the three water inflows can be the sole source that affects the river water quality.

The $\delta^{34}S_{sulfate}$ values in the river (5–7‰) are similar to those of the three major water sources, the Zarqa River (9‰), the brines, and sulfate-rich groundwater (4–10‰; Table 2 and Fig. 3), and hence cannot be used to detect the relative contribution of these sources. The $^{87}Sr/^{86}Sr$ and $\delta^{11}B$ variations (Fig. 12) show that the brines and sulfate-rich groundwaters have similar $^{87}Sr/^{86}Sr$ ratios (0.7081) but differ in their $\delta^{11}B$ values as the

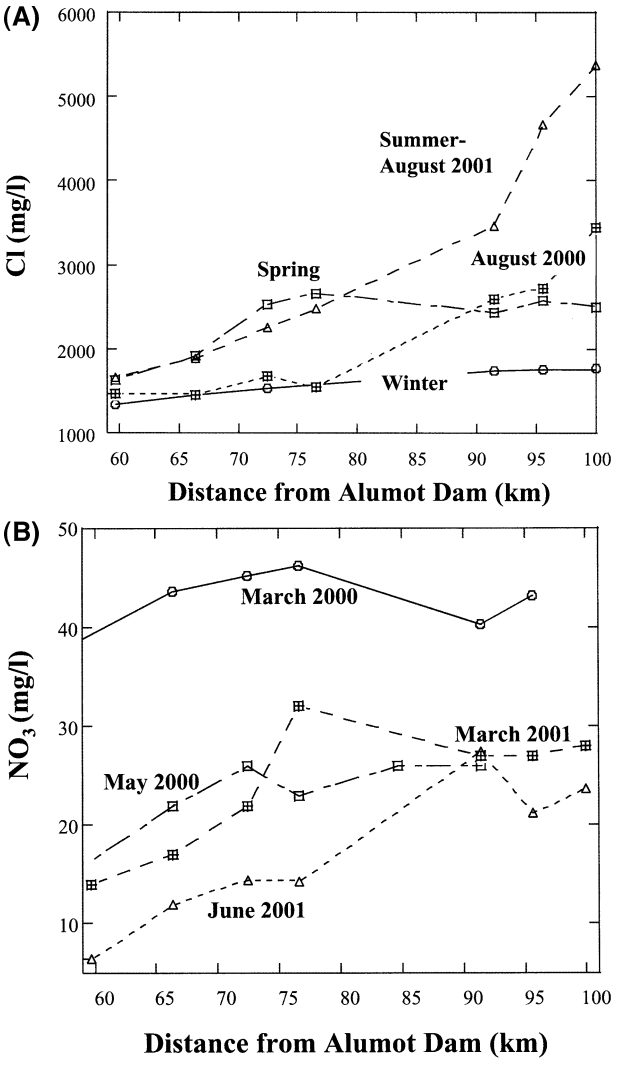

Fig. 9. The variation of chloride (A) and nitrate (B) contents (in mg/L) with flow distance along the southern Jordan River as recorded during winter, spring, and summer (sampled at 4 of 14 field trips).

brines are characterized by $\delta^{11}B>40‰$. In contrast, the Zarqa River has a high $^{87}Sr/^{86}Sr$ (0.7087) and low $\delta^{11}B$ (~25‰) values.

The constant downstream $\delta^{18}O_{water}$ values of the southern Jordan River (Fig. 3d) confirm that the rise of the salt content is not derived only from evaporation process, which would result in an increase of the $\delta^{18}O_{water}$. In contrast, all of the groundwater analyzed yielded low $\delta^{18}O_{water}$ values (<-4‰; Table 2). Hence, it seems that the $\delta^{18}O_{water}$ values recorded in the river reflect a balance between groundwater discharge (low $\delta^{18}O_{water}$) and residual evaporation (high $\delta^{18}O_{water}$).

Figure 13 illustrates that the salt content of the Jordan River is not derived from the individual saline inflows (i.e., brines or sulfate-rich groundwater) but rather from a saline groundwater that by itself is a mixture of the sulfate-rich groundwater and brines. The strontium ($^{87}Sr/^{86}Sr$~0.7081) and boron ($\delta^{11}B$~30‰) isotopic compositions of the Jordan River are also consistent with this interpretation. Given that the absolute salt concentration and chemical composition of this groundwater source is unknown, we used the ionic ratios measured for Jordan River water to estimate the chemical composition of this end member.

We hypothesize that the chemical composition of the groundwater that is discharged directly to the Jordan River lies along a mixing line between the brines and the sulfate-rich groundwater. Hence, we initially calculated the possible mixing line (Line 3 in Fig. 14) between these two sources. We used the highest chloride values and the average ionic ratios measured for the sulfate-rich groundwater and brines as proxies for these two water sources.

Subsequently we calculated possible mixing scenarios between the postulated groundwater source and the Jordan River water for the specific salinization events in the spring (Line 1 in Fig. 14) and summer (Line 2 in Fig. 14). Calculations were done separately for two areas: Zarzir-Tovlan sites in the north (60–72 km downstream from Alumot) and Allenby Bridge-Abdalla Bridge sites in the south (91–100 km (Fig. 2)). At each area we consider the northern site (Zarzir or Allenby Bridge) as the "upstream river" and the southern (and saline) sites (Tovlan or Abdalla Bridge) as the "downstream river." We employed mixing equations for different dissolved constituents (e.g., Cl^-, Na^+, SO_4^{2-}, Br^-), using the solute contents measured in the downstream river as the mixing products between the "upstream river" and an unknown saline "end member." The calculations point to a single solution for the mixing equations (M1 and M2 in Fig. 14), indicating a groundwater source with chloride of ~282 mM in Tovlan site (72 km) and ~564 mM in Abdalla site (100 km). Consequently, the estimated groundwater contribution to the Jordan River based on the solute mass balance in both sites is ~10%. It should be noted that our calculations show that the chemical composition of the groundwater inflows are different at the two sites. At the northern site, the mixed end member (Cl~282 mM; M1 in Fig. 14) is characterized by higher Na/Cl and SO_4/Cl ratios and reflects a mixture of 88% of saline groundwater with 12% brine. At the southern site, the higher salt content of the postulated mixing end member (Cl~564 mM; M2 in Fig. 14) reflects a larger fraction of brine, e.g., 60% groundwater and 40% brine. Since the groundwater and the brine differ in their $\delta^{11}B$ values (~30‰ and >39‰, respectively) we tested the mixing calculations using boron isotopic systematics. The available $\delta^{11}B$ values determined for the Tovlan site (30–32‰) are consistent with the expected $\delta^{11}B$ range upon mixing calculations made for the major dissolved solutes. We conclude that the volume contribution of the groundwater discharge to the Jordan River is low (10%), but due to the high salt content of this source its impact on the water quality of the Jordan River is significant. Consequently, the dissolved salts of the southern end of the Jordan River are controlled by the relationship between the seasonally variable surface discharge and the relatively constant groundwater inflow. In the winter, a surface discharge of ~1660 L/s corresponds to a chloride content of ~56 mM whereas in the summer a significant drop in the river discharge (370 L/s; Holtzman, 2003) results in increasing chloride content up to 152 mM (Tovlan site).

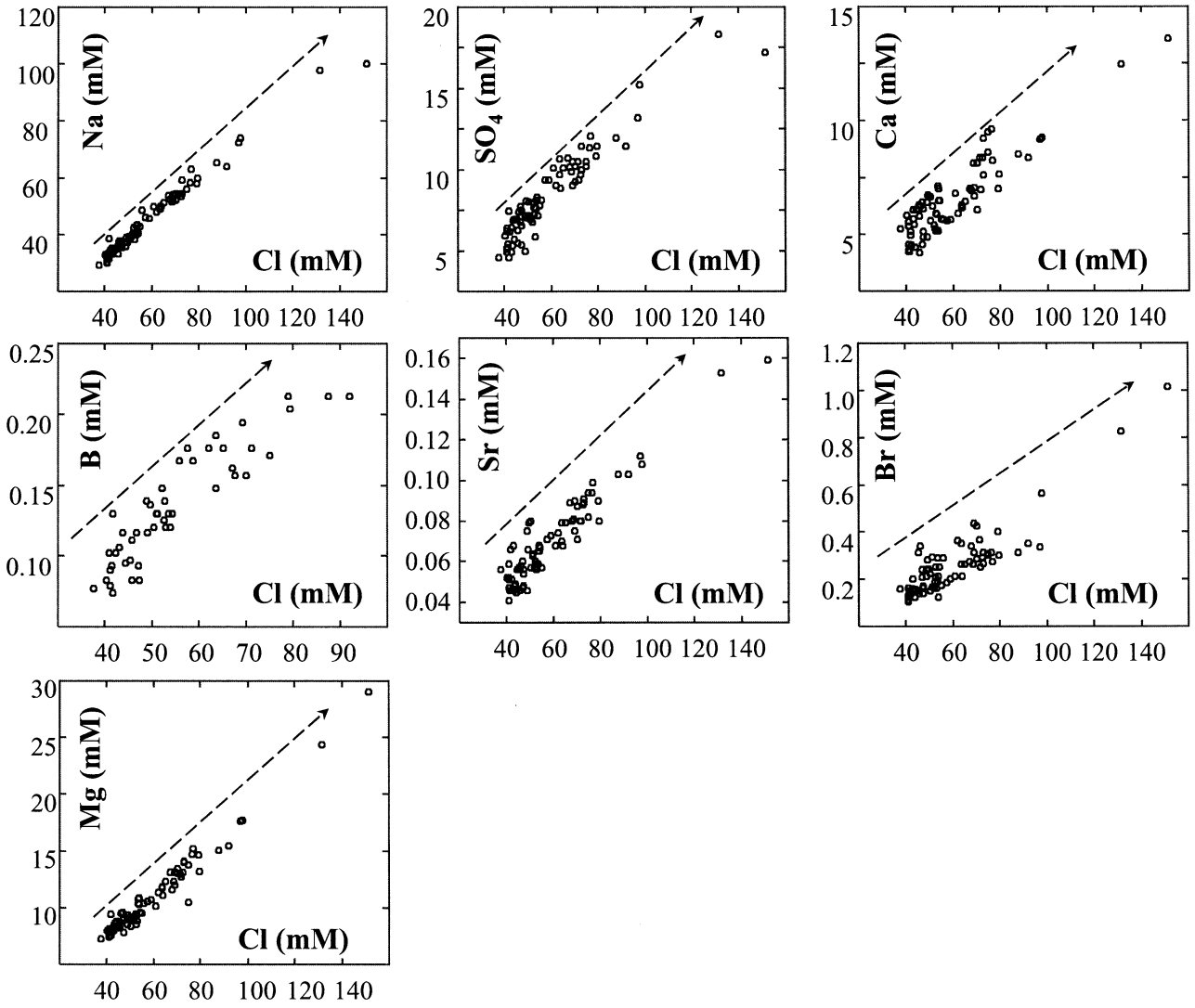

Fig. 10. Major elements versus of chloride content in the southern Jordan River. The arrow represents the flow direction of the river. Note the linear relationships between most of the dissolved salts and chloride, indicating that mixing controls the water quality of the Jordan River.

4.5. Sources of Dissolved Salts in Groundwater in the Southern Jordan Valley

We suggest that the sulfate-rich groundwater is derived from leaching of Pleistocene and Neogene sediments in the Jordan Valley (Fig. 1). The groundwater flows within the Lisan and Samra Formations, in which the Jordan River is incised. Landmann et al. (2002) extracted solutions from these sediments in the southern Jordan Valley that yielded SO_4/Cl and Br/Cl ratios of 0.5 and 1.9×10^{-3}, respectively. Similar ratios were observed for the saline groundwater. The relatively low Br/Cl ratio ($\sim 2 \times 10^{-3}$) indicates halite dissolution, which can explain the relatively high Na/Cl (0.8–1.0) in the saline groundwater. Furthermore, the δ^{11}B values (~30‰) and $^{87}Sr/^{86}Sr$ ratios (between 0.70802 to 0.70822) in the groundwater (Fig. 12) mimic those of the Lisan Formation (M. Stein, private communication; Stein et al., 1997). The δ^{11}B value of ~30‰ suggests that carbonate dissolution is the dominant boron source in the groundwater, although we can not rule out gypsum contribution with a similar δ^{11}B value. While marine carbonate minerals have δ^{11}B values of ~20‰, which reflects isotopic fractionation in the magnitude of ~20‰ relative to seawater (Vengosh et al., 1991b), it seems that the relatively higher δ^{11}B values in the Lisan Formation reflect a high δ^{11}B value in the parent brines, from which carbonate or gypsum were precipitated. Indeed higher δ^{11}B values (>39‰) are typical for Dead Sea brines (Vengosh et al., 1991a) as observed also in the Ca-chloride brines in our study. In contrast, the $\delta^{34}S_{sulfate}$ values of the sulfate-rich groundwater (4–10‰) are different from that of primary gypsum layers in the Lisan Formation (14–28‰; Gavrieli et al., 1998). However, disseminated (secondary) gypsum within the aragonites of the Lisan Formation has negative δ^{34}S values (down to −26‰; Gavrieli et al., 1998) and therefore the observed $\delta^{34}S_{sulfate}$ values of the groundwater may represent mixing of these two sulfate sources

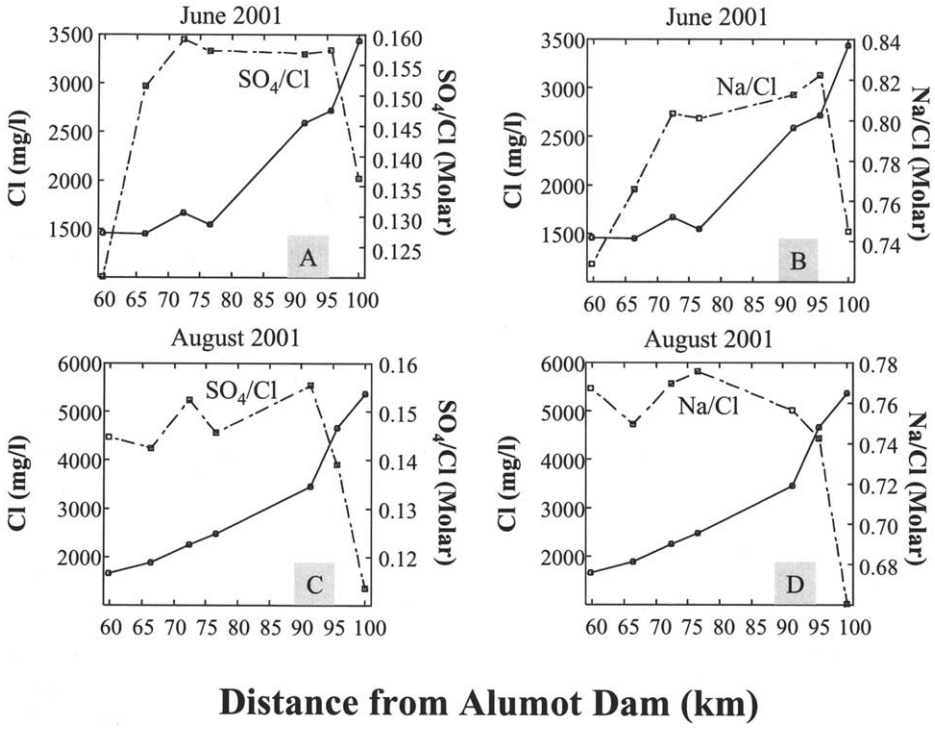

Fig. 11. Chloride (mg/L), SO_4/Cl, and Na/Cl ratios transects along the southern Jordan River sampled during June and August 2001. Note the different chemical composition of the river before and after a distance of ~90 km from Alumot Dam.

within the Lisan Formation. In contrast to the sulfate-rich groundwater, the brine composition is typical of groundwater in the Rift Valley (e.g., low Na/Cl high Br/Cl ratios) and reflects different stages in the evolution of the Dead Sea brines (Starinsky, 1974; Yechieli et al., 1996; Stein et al., 1997). Yet, their

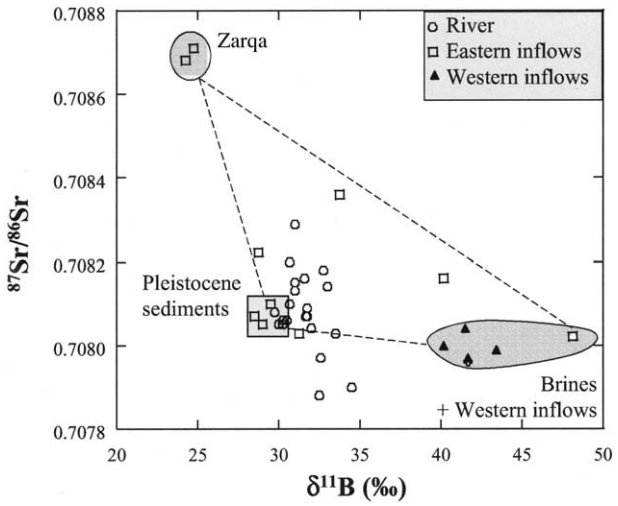

Fig. 12. $^{87}Sr/^{86}Sr$ versus $\delta^{11}B$ ratios of the southern Jordan River and the three major sources in the southern Jordan Valley. Note the relatively high $^{87}Sr/^{86}Sr$ ratios and low $\delta^{11}B$ in the Zarqa River, which has only minor impact on the composition of the Jordan River. The isotopic composition of the Pleistocene (Lisan) sediments (data from Stein et al., (1997)) controls the composition of both the sulfate-rich groundwater and the Jordan River.

$\delta^{34}S_{sulfate}$ values are lower compared to those of typical Ca-chloride brines (usually around 20‰), suggesting some additional input of ^{34}S depleted sulfate.

Geophysical surveys of groundwater in the Jericho area (Gropius and Klingbeil, 1999) have suggested that brine occupies the deepest part of the Pleistocene sediments at a depth of ~80 m, and is overlain by less-saline groundwater. The chemistry of groundwater in the Jericho area indeed reflects a mixture of these two water sources (Marie and Vengosh, 2001). We suggest that in the upper section of the southern Jordan River, from of 60 to 80 km, the location of the interface between the less-saline groundwater and the brines is relatively deep, and thus the groundwater contribution to the mixing product is higher (i.e., the river receives a larger fraction of the sulfate-rich groundwater). Further south, the depth of the interface is probably shallower and hence the brine contribution to the mixture that flows to the Jordan River is significantly higher. This explains why we observed the chemical variations in the southern section of the Jordan River (Fig. 11).

The southern part of the Jordan River is also characterized by a gradual increase of nitrate concentrations with flow distance (Fig. 9b) and $\delta^{15}N_{nitrate}$ values between 15‰ and 17‰ (Table 2). Similarly, the sulfate-rich groundwater is also characterized by high nitrate concentrations, particularly on the eastern side of the valley (up to 2.2 mM, Table 1). We suggest that the sulfate-rich groundwater is derived from agricultural drainage water that flows through the Pleistocene sediments where they induce dissolution of the saline marls and gypsum. The high nitrate concentrations in these waters are a result of extensive agricultural activities in the southern Jordan valley, which has

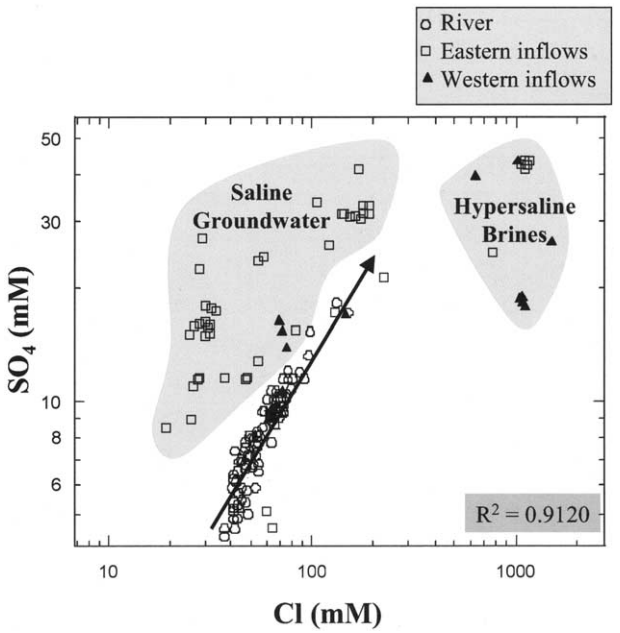

Fig. 13. Log sulfate versus log chloride contents of the Jordan River as compared to the sulfate-rich groundwater and brines. Arrow represents the river flow direction. Note that the linear relationship between Cl^- and SO_42 contents in the Jordan River was obtained in a linear scale. The log-log presentation illustrates that the saline source that controls the river salt content is, by itself, a mixing product between the brines and the sulfate-rich groundwater.

been extensively irrigated during the last decade. A large fraction of the irrigation water in the southern Jordan Valley is derived from wastewater from Amman, Jordan. At the eastern side of the Jordan Valley, ~30 to 40 MCM of treated wastewater is annually blended with ~10–20 MCM of fresh water from King Abdalla Canal (originally from the fresh Yarmouk River) and used for irrigation (a total of ~60 MCM/yr; Shatanawi and Fayyad, 1996). On the western side of the valley, an addition of ~30 MCM/yr is used for irrigation of agricultural fields. Increasing nitrate concentrations along the Jordan River (Fig. 9b) coupled with high $\delta^{15}N_{nitrate}$values (15–17‰) indicate a significant influx of agricultural return flow triggered by irrigation with wastewaters. We further conclude that the extensive irrigation over the flood plains of the Jordan River enhances dissolution and leaching of sediments that together with underlying brines control the salt content of shallow groundwater that is discharged into the Jordan River.

CONCLUSIONS

Although river salinization phenomena have been reported for major river basins such as the Colorado River (Pillsbury, 1981), Arkansas River (Gates et al., 2002), Nile River (Kotb et al., 2000), the Euphrates and Tigris rivers in Iraq (Fattah and Abdul Baki, 1980; Robson et al., 1983), and the Murray River (Allison et al., 1990; Herczeg et al., 1993), only few studies (Herczeg et al., 1993; Phillips et al., 2002) have used geochemistry and isotopic systematics to elucidate the sources of solutes that affect river quality. Indeed, different sources of salts have been postulated for river salinization. In the Murray-Darling Basin in South Australia soluble aerosols derived from the ocean are deposited in the drainage basin, concentrated by evapotranspiration, and discharged to the Murray River (Allison et al., 1990; Herczeg et al., 1993). In contrast, the riverine salts can also be derived from leaching of evaporitic rocks as demonstrated in the southern Rio Grande Basin, United States (Phillips et al., 2002).

The data presented in this study indicate that integration of several geochemical and isotopic tracers is essential in distinguishing the multiple sources that can affect the salt content of river systems. In particular, the distinction between natural groundwater discharge and anthropogenically induced agricultural return flow is important for basin management. Our findings suggest that the relative proportions of agricultural return flows in a river basin can vary significantly. Moreover, the relative contribution of saline water derived from leaching of sediments and from mixing with formation water varies dependent on hydrological conditions.

Our results revealed three distinct zones of salt content changes along the Lower Jordan River. Integration of hydrological, chemical, and isotopic (strontium, boron, sulfur, oxygen, nitrogen) data from the Jordan River and its tributaries enabled us to elucidate the different sources that control the water quality of the Jordan River. Using solute mass balances we were able to show that none of the identified tributary inflows can be a sole source for the high dissolved salts of the Jordan River. Instead, the water quality of the Jordan River is controlled to a large degree by groundwater discharge.

In the northern section, we estimate that the groundwater contribution varies between 20 to 50%. The discharge of the shallow sulfate-rich groundwater affects the quantity and water quality of both the Yarmouk (down flow from Adassia Dam) and Jordan rivers. Chemical and isotopic data suggest that the shallow groundwater is derived from a blend of agricultural drainage water, groundwater flow from the eastern tributaries

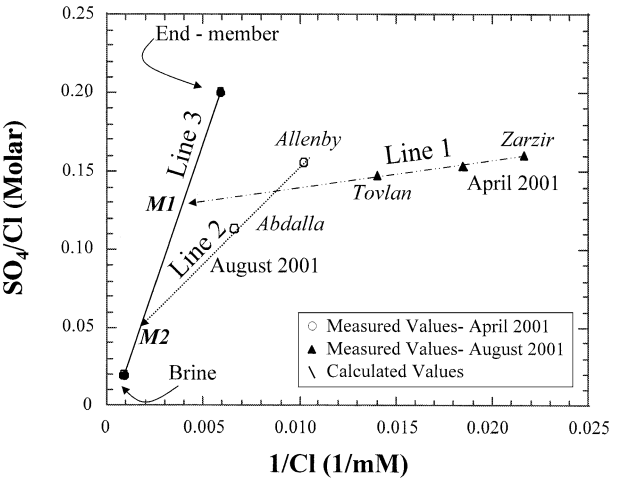

Fig. 14. SO_4/Cl ratios versus the reciprocal of chloride in two salinization events of spring (Line 1) and summer (Line 2) along two segments in the southern Jordan River (see locations in Figure 2). Line 3 represents the mixing relationships between the hypersaline brines (Cl=1128 mM) and sulfate-rich groundwater (Cl=169 mM). Note that the chemical data measured in the river is used to constrain possible saline groundwater end members, M1 in spring and M2 in summer, which are discharged and affect the salt content of the river.

(with low $\delta^{34}S_{sulfate}$ <0‰), and an unknown saline source with a low $^{87}Sr/^{86}Sr$ ratio (<0.7072). Alternatively, the agricultural return flow may be modified by addition of fertilizers with low $^{87}Sr/^{86}Sr$ values.

In the southern section of the Lower Jordan River we observed seasonal salinization events during the spring (TDS up to 6 g/L at a flow distance of 70–80 km) and summer (up to 11 g/L at the southern end of the river). We characterized the chemical and isotopic compositions of three major sources (1) the Zarqa River; (2) sulfate-rich saline groundwater; and (3) subsurface brines. We show that none of these sources can solely explain the salinization trend in the Jordan River, but that variable mixtures of the two latter can explain the chemical variations observed in the Jordan River. We used the chemical variations in the river to constrain the mixing proportions of these two sources and consequently derived possible mixing relationships between the discharged groundwater and the river. Our mixing simulations show that the groundwater that flows into the southern Jordan River is saline (chloride between 282–564 mM). Although the contribution of the groundwater to the Jordan River is estimated as only ~10%, its impact on its salt content is significant. The increase of nitrate concentrations with flow in the southern Jordan River, coupled with the high nitrate concentrations in the sulfate-rich groundwater suggest that the groundwater originates from agricultural drainage waters that flow through the Pleistocene sediments and trigger dissolution of the reactive saline sediments. Hence, although the sources of salts that flow to the Jordan River are geogenic, the magnitude of groundwater discharge depends on irrigation practices and thus agricultural activity in the Jordan Valley.

Our data show that the water quality of the Jordan River has deteriorated due to a combination of significant reduction of the annual flow (from ~1300 MCM to 50–200 MCM), dumping of diverted saline springs and wastewater, and discharge of shallow saline groundwater. Our mass balance calculations show that in the northern section the groundwater component is high (20 to 50% of the river flow) whereas in the southern section it is relatively low (~10%). Nevertheless, the southern Jordan River is much more saline due to an increased component of brine and the reactivity of the saline host sediments.

The impact of the groundwater component on the quality of the Jordan River is a major constraint for future management of the river and implementation of the Peace Treaty between Israel and Jordan (e.g., elimination of untreated sewage effluents, desalination of the saline water that composes the initial base flow, equal pumping rights to Israelis and Jordanians; Israel-Jordan Peace Treaty (1994)). Future elimination of the saline water and sewage at its source and further exploitation of the river, as suggested in the peace treaty, will increase the impact of the groundwater component and result in further deterioration of the ecological system. Salt levels will increase beyond the upper limit acceptable for fishponds recharge and irrigation of crops such as palm trees. This will have severe ramifications for the region's future economic livelihood, political stability, and cultural importance.

Acknowledgments—This study was supported by the U.S. Agency for International Development; Bureau for Global Programs, Field Support and Research; Center for Economic Growth and Agriculture Development, The Middle East Regional Cooperation program (MERC project M20–068). We thank ECO Jordan and the Nature Protection Authority in Israel for their field assistance and contribution. We also thank and appreciate the thorough and thoughtful reviews of the Associate Editor K. Falkner, W. M. Edmunds, W.F. Leaney, and an anonymous reviewer.

Associate editor: K. K. Falkner

REFERENCES

Allison G. B., Cook P. G., Barnett S. R., Walker G. R., Jolly I. D., and Hughes M. W. (1990) Land clearance and river salinization in the western Murray basin, Australia. *J. Hydrol.* **119,** 1–20.

Bajjali W., Clark I. D., and Fritz P. (1997) The artesian thermal groundwaters of northern Jordan: insights into their recharge history and age. *J. Hydrol.* **192,** 355–382.

Beaumont P. (1996) Agricultural and environmental changes in the upper Euphrates catchment of Turkey and Syria and their political and economic implications. *Appl. Geog.* **16,** 137–157.

Begin Z. B., Erlich A., Nathan Y. (1974) Lake Lisan–The Pleistocene precursor of the Dead Sea. *Geol. Surv. Isr. Bulletin* **63,** 1–30.

Bentor Y. K. (1961) Some geochemical aspects of the Dead Sea and the question of its age. *Geochim. Cosmochim. Acta* **25,** 239–260.

Böhlke J. K. and Horan M. (2000) Strontium isotope geochemistry of ground waters and streams affected by agriculture, Locust Grove, Maryland. *Applied Geoch.* **15,** 599–609.

Bullen T. D., Krabbenhoft D. P., and Kendall C. (1996) Kinetic and mineralogic controls on the evolution of groundwater chemistry and $^{87}Sr/^{86}Sr$ in a sandy silicate aquifer, northern Wisconsin, USA. *Geochim. Cosmochim. Acta* **60,** 1807–1821.

Coleman M. L. and Moore M. P. (1978) Direct reduction of sulfate to sulfur dioxide for isotopic analysis. *Anal. Chem.* **50,** 1594–1595.

Craig H. (1961) Standard for reporting concentrations of deuterium and oxygen-18 in natural waters. *Science* **133,** 1833–1834.

Cullen H. M., deMenocal P. B., Hemming S., Hemming G., Brown F. H., Guildeson T., and Sirocko F. (2000) Climate change and the collapse of the Akkadian empire: Evidence from deep sea. *J. Geol.* **28,** 379–382.

deMenocal P. B. (2001) Cultural responses to climate change during the Late Holocene. *J. Sci.* **292,** 667–669.

Exact (1998) Overview of Middle East Water Resources: Water resources of Palestinian, Jordanian and Israeli interest. Jordanian Ministry of Water and Irrigation, Palestinian Water Authority and Israeli Hydrological Service. A Report *Compiled by the U.S. Geological Survey for the Executive Action Team, Middle East Water Data Banks Project*.

Fattah Q. N. and Abdul Baki S. J. (1980) Effects of drainage systems on water quality of major Iraqi rivers. *Internat. Asso. Hydrol. Sci. Publ.* **130,** 265–270.

Gavrieli I., Stein M., Kolodny Y., and Spiro B. (1998) Sulfur isotopes in gypsum as indicator for paleolimnological conditions of Lake Lisan, the Dead Sea Rift Valley. *Am. Geophys. U. Annul. Fall Meet.*, San Francisco, December, 1958 p. F521.

Gavrieli I., Yechieli Y., Halicz L., Spiro B., Bein A., and Efron D. (2001) The sulfur system in anoxic subsurface brines and its implication on brine evolutionary pathways: The Ca-chloride brines in the Dead Sea area. *Earth Planet. Sci. Lett.* **186,** 199–213.

Gates T. K., Burkhalter J. P., Labadie J. W., Valliant J. C., and Broner I. (2002) Monitoring and modelling flow and salt transport in a salinity-threatened irrigated valley. *J. Irrig. Drain. Eng. Asce.* **128,** 87–99.

Gropius M. and Klingbeil R. (1999) Hydrogeological and geophysical investigation in Jericho area. DGG-Meeting on Environmental Geophysics, Neustadt, Germany. p. 8.

Hazan N. (2003) Reconstruction of Kinneret Lake. Levels in the last 40,000 years. Master's thesis, the Hebrew University of Jerusalem.

Herczeg A. L., Simpson H. J., and Mazor E. (1993) Transport of soluble salts in a large semi-arid basin: River Murray, Australia. *J. Hydrol.* **144,** 59–84.

Hem J. D. (1985) Study and interpretation of the chemical characteristics of natural water. <*http://water.usqs.gov/pubs/wsp2254/*> *U.S. Geol. Surv. Water-Supply Paper* **2254**.

Hof F. C. (1998) Dividing the Yarmouk's waters: Jordan's treaties with Syria and Israel. *Water Policy* **1,** 81–94.

Holtzman R. (2003) Salinization sources along the Lower Jordan River under draught conditions. Master's thesis, Technion (in Hebrew).

Israel-Jordan Peace Treaty, Annex II, Water Related Matters (1994) (http://www.us-israel.org/jsource/Peace/annex2.html).

Klein M. (1998) Water balance of the Upper Jordan River basin. *Water Inter.* **23,** 244–248.

Kolodny Y., Katz A., Starinsky A., Moise T., and Simon E. (1999) Chemical tracing of salinity sources in lake Kinneret (Sea of Galilee), Israel. *Limnol. Oceanog.* **44,** 1035–1044.

Kotb T. H. S., Watanabe T., Ogino Y., and Tanji K. T. (2000) Soil salinization in the Nile Delta and related policy issues in Egypt. *Agri. Water Manag.* **43,** 239–261.

Landmann G., Abu Qudaira G. M., Shawabkeh K., Wrede V., and Kempe S. (2002) Geochemistry of the Lisan and Damya Formation in Jordan, and implications for paleoclimate. *Quaternary Inter.* **89,** 45–57.

Marie A. and Vengosh A. (2001) Sources of salinity in groundwater from Jericho area, Jordan valley. *J. Ground Water* **39,** 240–248.

Möller P., Rosenthal E., Dulski P., Geyer S., and Guttman Y. (2003) Rare earths and yttrium hydrostratigraphy along the Lake Kinneret-Dead Sea-Arava transform fault, Israel and adjoining territories. *Applied Geoch.* **18,** 1613–1628.

Neev D. and Emery K. O. (1967) The Dead Sea. *Isr. Geol. Sur. Bulletin* **41,** 147 pp.

Phillips F. M., Hogan J. F., Mills S. K., and Hendrickx J. M. H. (2002) Environmental tracers applied to quantifying causes of salinity in arid-region rivers: preliminary results from the Rio Grande, Southwestern USA. In *Development in Water Science, Vol 50*. Water Resources Perspectives: Evaluation, Management and Policy (eds. Alsharhan A. S. and Wood W. W.). Elsevier, Amsterdam.

Pillsbury A. F. (1981) The salinity of rivers. *Sci. Am.* **245,** 54–65.

Robson J. F., Stoner R. F., and Perry J. H. (1983) Disposal of drainage water from irrigated alluvial plains. *Water Sci. Tech.* **16,** 41–55.

Rosenthal E. (1987) Chemical composition of rainfall and groundwater in recharge areas of the Bet Shean-Harod multiple aquifer system, Israel. *J. Hydrol.* **155,** 329–352.

Salameh E. (1996) Water quality degradation in Jordan. Friedrich Ebert Stiftuns and Royal Society for Conservation of Nature, Amman, Jordon. 179 pp.

Salameh E. and Naser H. (1999) Does the actual drop in Dead Sea level reflect the development of water resources within its drainage basin. *Acta Hydrochim. Hydrobiol.* **27,** 5–11.

Segal M., Shavit U., Holtzman R., Farber E., Gavrieli I., Bullen T., Mayer B., Shaviv A., and Vengosh A. (in press) Nitrogen pollutants, sources and processes along the Lower Jordan River. *J. Envromn. Qual*.

Shatanawi M. and Fayyad M. (1996) Effect of Khirbet As-Samra treated effluent on the quality of irrigation water in the central Jordan Valley. *Water Res.* **30,** 2915–2920.

Shavit U., Holtzman R., Segal M., Vengosh A., Farber E., Gavrieli I., Bullen T., and ECO-Research Team (2002) *Water Sources and Quality Along the Lower Jordan River, Regional Study, in Water Resources Quality, Preserving the Quality of our Water Resources* (ed. H. Rubin et al.), pp. 127–148, Springer-Verlag.

Silva S. R., Kendall C., Wilkison D. H., Ziegler A. C., Chang C. C. Y., and Avanzino R. J. (2000) A new method for collection of nitrate from fresh water and analysis of the nitrogen and oxygen isotope ratios. *J. Hydrology* **228,** 22–36.

Starinsky A. (1974) Relationship between Ca-chloride brines and sedimentary rocks in Israel. Ph.D thesis, Hebrew University.

Stein M., Starinsky A., Katz A., Goldstein S. L., Machlus M., and Schramm A. (1997) Strontium isotopic, chemical, and sedimentological evidence for the evolution of lake Lisan and the Dead Sea. *Geochim. Cosmochim. Acta* **61,** 3975–3992.

Vengosh A., Starinsky A., Kolodny Y., and Chivas A. R. (1991a) Boron-isotope geochemistry as a tracer for the evolution of brines and associated hot springs from the Dead Sea, Israel. *Geochim. Cosmochim. Acta* **55,** 1689–1695.

Vengosh A., Kolodny Y., Starinsky A., Chivas A. R., and McCulloch M. T. (1991b) Coprecipitation and isotopic fractionation of boron in modern biogenic carbonates. *Geochim. Cosmochim. Acta* **55,** 2901–2910.

Waldmann N. (2002) The geology of the Samra Formation in the Dead Sea Basin. Master's thesis, The Hebrew University of Jerusalem.

Williams W. D. (2001) Anthropogenic salinization of inland waters. *J. Hydrobiol.* **466,** 329–337.

Yechieli Y., Gavrieli I., Berkowitz B., and Ronen D. (1998) Will the Dead Sea die? *Geology* **26,** 755–758.

Yechieli Y., Ronen D., and Kaufman A. (1996) The source and age of groundwater brines in the Dead Sea area, as deduced from ^{36}Cl and ^{14}C. *Geochim. Cosmochim. Acta* **60,** 1909–1916.